Quantification of Biogenic Turbulence

Stephen Camozzi

Master of Engineering

Department of Mechanical Engineering

McGill University

Montréal, Québec

August 2017

A thesis submitted to McGill University in partial fulfillment of the requirements of the degree of Master of Engineering.

DEDICATION

This thesis is dedicated to those teachers who have inspired my passion for science and engineering, especially Louis Blizzard, as well as the many friends and family who have fostered my love of nature and the sea.

ACKNOWLEDGEMENTS

The opportunity to contribute to experimental engineering and ocean science research has made for an often challenging, though tremendously formative and fulfilling experience. Such an opportunity would not have been possible without the unwavering trust, support and encouragement of my supervisors, Professor Laurent Mydlarski and Professor Susan Gaskin, and I am also appreciative of the independance they have afforded me in my studies. In addition, I owe a great deal of my understanding of and interest in turbulence to Professor Mydlarski. This work would also not have been possible without the tremendous support provided by the many non-academic staff members at McGill, especially John Bartczak and the Civil Engineering staff, Fernando Chaurand, and the Animal Care team. Thanks are also due to Jeanette Frandsen and Régis Xarde from the INRS Centre Eau Terre Environnement, for their generous loan of the Nortek Vectrino Profiler. The good humour and helpful hands of my colleagues and friends in the hydraulics and aerodynamics labs (often those of Max Milanovic) have also made for an enjoyable and memorable past three years, especiaclly Yulia Akutina and Alejandro Perez-Alvarado, who welcomed me in the lab and helped guide me through the experimental process. Of course, finding success and fulfillment in my passion for science and learning owes a great deal to the support and friendship of my family, classmates, teachers and teammates I have had the pleasure to know over these past years and throughout my life. Finally, a very special thank you to Ema for your love and support throughout this journey.

ABSTRACT

The processes through which the ocean dissipates internal energy and maintains circulation continue to present oceanographers and other scientists with a complex set of research problems and questions. Excluding the first suggestion, and subsequent dissmissal, of the potential role of biollogically-generated (biogenic) turbulence in the 1960s [Munk, 1966], recent theoretical estimates and field measurements have stirred debate over the potential role of biogenic turbulence in oceanic energy dissipation and circulation. However, the results of these studies have spanned orders of magnitude, particularly in their estimation of the dissipation rate of turbulent kinetic energy, thus leaving little consensus over the relative importance of biogenic turbulence. In an effort to inform this debate, controlled, laboratory experiments have been conducted to measure turbulence parameters within schools of two species of tropical fish, namely Congo and neon tetras, using an acoustic Doppler velocimeter (ADV). This study was designed to address questions relating to the structure of biogenic turbulence, the biological factors affecting it, and its corresponding significance in the ocean. Additionally, seperate validation experiments were conducted in a turbulent jet, to characterize and compare the performances of single-point and profiling ADVs, both with each other and accepted literature data. These experiments demonstrated consistency between the two ADVs in their ability to accurately measure turbulence, and, most importantly, dissipation rates. The experiments with fish i) served to verify the assumption that biogenic turbulence is approximately isotropic [Katija, 2012], ii) revealed the independence of biogenic turbulence parameters and abundance (or aggregation density), and iii) indicated a relationship with animal body size. The dissipation rate corresponding to the Congo tetras was $O(10^{-5} - 10^{-4})$ W kg^{-1}, comparable to that observed in the upper ocean, attributed to the effects of surface winds, while that corresponding to the neon tetras was $O(10^{-7} - 10^{-6})$ W kg^{-1}, near the upper bound of the dissipation rate observed in the abyssal and strongly stratified regions of the ocean. These results demonstrate the potential importance of biogenic turbulence to

ocean dynamics. This work was carried out under McGill standard operating procedures for the ethical use of animals, according to Protocol #2014-7505.

SOMMAIRE

Les processus par lesquels l'océan dissipe l'énergie interne et maintient la circulation continuent de présenter un ensemble complexe de problèmes de recherche et de questions aux océanographes et d'autres scientifiques. Pour la première fois depuis la suggestion originale du rôle potentiel de la turbulence biogénique dans les années 1960 qui fût ensuite rejetée, [Munk, 1966], des estimations théoriques récentes et des mesures océaniques ont provoqué un débat sur le rôle potentiel de la turbulence biogène dans la dissipation d'énergie et la circulation océanique. Cependant, les résultats de ces études ont couvert plusieurs ordres de grandeur, en particulier dans leur estimation du taux de dissipation de l'énergie cinétique turbulente, ce qui remet en question l'importance relative de la turbulence biogénique. Dans le but de clarifier ce débat, des expériences de laboratoire contrôlées ont été menées pour mesurer les paramètres de turbulence dans les banques de deux espèces de poissons tropicaux, savoir le tétra du Congo et le tétra néon, en utilisant un velocimètre acoustique Doppler (ADV). Cette étude a été conçue pour répondre aux questions relatives à la structure de la turbulence biogénique, aux facteurs biologiques qui l'affectent et à son importance dans l'océan. En outre, des expériences de validation ont été menées séparément dans un jet turbulent, pour caractériser et comparer les performances des ADV à point unique et de profilage, à la fois entre l'un et l'autre ainsi qu'avec les données de la littérature acceptée. Ces expériences ont démontré la cohérence entre les deux ADV dans leur capacité à mesurer avec précision la turbulence et, surtout, les taux de dissipation. Les expériences avec les poissons i) ont servi à vérifier l'hypothèse selon laquelle la turbulence biogénique est quasi-isotrope [Katija, 2012], ii) ont révélé l'indépendance des paramètres de turbulence biogénique et l'abondance (ou densité d'agrégation), et iii) ont indiqué une relation avec la taille du corps animal. Le taux de dissipation correspondant aux tétras du Congo était de $O(10^{-5} - 10^{-4})$ W kg^{-1}, comparable à celui observé dans la couche supérieure des océans, qui est attribué aux effets des vents de surface. Le taux de dissipation correspondant aux tétras néon était

$O(10^{-7} - 10^{-6})$ W kg^{-1}, près de la limite supérieure du taux de dissipation observé dans les régions abyssales et fortement stratifiées des océans. Les résultats démontrent l'importance potentielle de la turbulence biogénique pour la dynamique des océans. Ce travail a été effectué dans le cadre des procédures d'exploitation standards de McGill pour l'utilisation éthique des animaux, selon le Protocole #2014-7505.

TABLE OF CONTENTS

LIST OF TABLES

LIST OF FIGURES

CHAPTER 1
Introduction

1.1 Motivation

For explorers and scientists alike, from Jacques Cousteau to Sir David Attenborough and thousands of dedicated researchers across the globe, the world's oceans were, and remain, one of the last great frontiers of our planet. Humanity's knowledge gap in the marine sciences also encompasses a lack of understanding regarding the role of the biosphere in the fluid dynamics underlying many oceanic processes. Recently, however, processes such as turbulent energy dissipation from swimming animals [Huntley and Zhou, 2004, Dewar et al., 2006], large-scale fluid motions due to the vertical migration of animal aggregations [Wilhelmus and Dabiri, 2014], and dissolved oxygen dispersion within schools of fish [Plew et al., 2015], have received attention as possible contributors to ocean energy dynamics, vertical mixing, and ecosystem management. Specifically, biologically-generated (biogenic) turbulence, namely the chaotic fluid motions induced by the movements of animals, may be an important, though complicating factor in the development of ocean models and theory at various scales. Although, biogenic turbulence was wholly ignored in the context of mixing and the ocean energy budget, shortly after its first consideration by Munk (1966), preliminary work (including that mentioned above) over the past decades has elucidated its potential impacts.

Although the foundational concepts surrounding biogenic turbulence are relatively straightforward (i.e. fish overcome fluid drag to propel themselves, thereby transferring energy to the surrounding fluid and producing a turbulent wake), determining its precise impact is complicated by the combined effects of animal behaviour, morphology, meteorology, and various other factors. Due, in part, to such complexities, as well as a lack of repeatable experimental data, a debate over the importance of biogenic turbulence, sparked after early work on the

topic, remains ongoing. Although more recent work has proved intriguing, or helped to suggest possible species inducing significant biogenic turbulence, there is a need for data from controlled, laboratory experiments to better inform this debate. Through the acquisition of baseline measurements of biogenic turbulence within aggregations of animals, particularly those swimming in the intermediate-high Reynolds number regime, necessary conditions for substantial or non-negligible biogenic turbulence may be identified. Furthermore, the systematic quantification of biogenic turbulence is necessary for a more accurate understanding of our oceans, or more broadly, the role of marine life, and its exploitation by humans, in determining the function of ocean processes, and by extension, our climate.

1.2 Objectives

Given the need for controlled laboratory measurements of biogenic turbulence, an experimental study has been undertaken to quantify the turbulence within schools of two fish species, over a range of abundances, or levels of aggregation density. This study sought to provide controlled measurements with which the nature and relative importance of biogenic turbulence could be assessed, while using a procedure that could be extended to a wider variety of species and animal behaviours. First, the experiments described herein aimed to test the validity of the generally held assumptions that biogenic turbulence is isotropic and similar in structure to physically-induced turbulence. Furthermore, to study the effects of animal size and abundance on biogenic turbulence and compare these laboratory measurements to theoretical predictions, on an order of magnitude basis. Lastly, to compare the results to characteristic data of ocean background turbulence to further the understanding of the role of biogenic turbulence in the real-world environment. A secondary objective of this work was to evaluate the performance of two acoustic Doppler velocimeters (ADVs), particularly their ability to measure the dissipation rate, through validation experiments in a turbulent jet. Through these objectives, a framework for continued investigations into biogenic turbulence, focused on variations in animal species and behaviours, using ADVs, has been developed. The intended continuation of this work may eventually allow for the accurate prediction of

biogenic turbulence parameters and its incorporation into models of ocean mixing and energy dissipation.

1.3 Literature review

Over the past decades, extensive theoretical and experimental research has been devoted to the study of turbulence in the ocean, and to a greater extent, the fundamental physics underlying turbulent motion. The quantity of related literature is correspondingly vast, thus, this review will encompass the theoretical background necessary for the analysis of biogenic turbulence, as measured in this study, as well as those works which have served as an inspiration for the study of biogenic turbulence/mixing and contributed to its understanding. For a broader summary of ocean turbulence, Thorpe (2005, 2007) provides rigorous and introductory texts, respectively, while Tennekes & Lumley (1972) and Pope (2000) provide complementary and comprehensive texts on turbulence fundamentals.

1.3.1 Turbulence theory

The overwhelming majority of fluid motion observed in nature falls into the regime of turbulent flow, whether it be the large scale motion of an ocean current or the wake produced by a swimming fish. Although exceedingly common, turbulence remains one of the last unsolved problems of classical physics and lacks a single concise definition. In general, definitions of turbulence are subjective, tending to focus on a particular characteristic of turbulent flows. It is better then to simply keep in mind some universal aspects of turbulence, such as its tendencies to be dissipative, random, and require a source of energy to sustain its motions. Additionally, turbulence is generally three-dimensional, has non-zero vorticity, and encompasses a range of scales. In the measurement and analysis of biogenic turbulence, it is imperative to recall some basic concepts of contemporary turbulence theory and their relation to the unique aspects of biogenic turbulence. Specifically, the mathematical theory underlying fluid motion, the application of statistical tools in turbulence (especially in regard to the rate of energy dissipation), the various scales of turbulent motion and their corresponding physics, and the spectral behaviour of homogeneous isotropic turbulence are of particular relevance.

In mathematical terms, turbulence is believed to correspond to the chaotic regime of the Navier-Stokes equations (a set of dynamical equations which govern fluid motion, to which no closed-form solution is known to exist), which are defined for constant-property, Newtonian fluids as:

$$\rho\frac{\partial u_j}{\partial t} + \rho\frac{\partial}{\partial x_j}(u_i u_j) = \frac{\partial \tau_{ij}}{\partial x_i} - \rho\frac{\partial \Psi}{\partial x_j}, \quad i,j = 1,2,3, \tag{1.1}$$

where Ψ is a gravitational potential and the viscous stress tensor τ_{ij} is defined as:

$$\tau_{ij} = -P\delta_{ij} + \mu\left(\frac{\partial U_i}{\partial x_j} + \frac{\partial U_j}{\partial x_i}\right), \tag{1.2}$$

where P is the pressure and μ is the dynamic viscosity [Pope, 2000]. After proper non-dimensionalization, the equations include a non-dimensional parameter, referred to as the Reynolds number, which can be considered a ratio of inertial to viscous forces and has the form:

$$Re = \frac{UL}{\nu}, \tag{1.3}$$

where U is a characteristic velocity of the fluid, L is a characteristic length scale, and ν is the kinematic viscosity of the fluid. In the context of biogenic turbulence, Re refers to an animal Reynolds number, where U is a characteristic swimming speed and L is generally the body length [Huntley and Zhou, 2004]. As Re increases, flows transition from the laminar to turbulent regime, eventually becoming fully turbulent and exhibiting behaviour characteristic of turbulence at sufficiently large Re. This critical value is approximately 10^5 for external flows (those over a swimming body for instance) and 2 300 for internal flows (through a pipe).

Lacking a complete mathematical description in the turbulent regime, researchers have relied on the implementation of statistical tools to quantify the behaviour of specific flows and the physical mechanisms underlying turbulent motion. Importantly, these methods provide insight into and allow for the quantification of the energy dynamics within turbulent flow and its effects on the surrounding environment. One of the first analytical steps is to consider instantaneous parameters describing such flows (velocity, pressure, etc.) as being comprised of a mean and fluctuating component, a notion defined as the Reynolds decomposition. For

velocity, the decomposition is of the form:

$$\tilde{u_i} = \overline{U_i} + u_i, \tag{1.4}$$

where $\tilde{u_i}$ is the instantaneous velocity, $\overline{U_i}$ the mean, and u_i the fluctuating component. Applying this decomposition to the conservation equations, it is clear that the number of variables required to fully define a mean turbulent flow is greater than the number of valid equations comprising the mean conservation laws. This recurring discrepancy is referred to as the closure problem. However, such exercises of manipulating conservation laws to derive "turbulent budgets" of various parameters can provide important insight into the dynamics and energetics of turbulence. For example, since it was previously stipulated that turbulence is inherently dissipative and requires a constant source of energy, it is useful to derive a turbulent kinetic energy budget, where the turbulent kinetic energy per unit mass (TKE) is defined as:

$$TKE = \frac{1}{2}\overline{(u_i u_i)} \tag{1.5}$$

In deriving the budget of TKE from the mean flow and Navier-Stokes equations, a viscous dissipation term arises, or more specifically, the rate of dissipation of TKE per unit mass (which is often simply referred to as the dissipation rate or ϵ). In its most general form, the dissipation rate is defined as:

$$\epsilon = \frac{1}{2}\nu\overline{\left(\frac{\partial u_i}{\partial x_j} + \frac{\partial u_j}{\partial x_i}\right)\left(\frac{\partial u_i}{\partial x_j} + \frac{\partial u_j}{\partial x_i}\right)} \tag{1.6}$$

Though in practical terms, the simultaneous measurement of nine spatial gradients of velocity is most often impossible. However, for locally homogeneous turbulence, the dissipation rate is:

$$\epsilon = 3\nu\left(\overline{\left(\frac{\partial u_1}{\partial x_1}\right)^2} + \overline{\left(\frac{\partial u_2}{\partial x_1}\right)^2} + \overline{\left(\frac{\partial u_3}{\partial x_1}\right)^2}\right), \tag{1.7}$$

which can be further simplified for homogeneous isotropic turbulence:

$$\epsilon = 15\nu\overline{\left(\frac{\partial u_1}{\partial x_1}\right)^2} \tag{1.8}$$

According to Taylor [Taylor, 1935] the dissipation rate may also be estimated by considering the balance between TKE production and dissipation by viscosity, resulting in the relation:

$$\epsilon = C_{\epsilon_1} \frac{u_{rms}^3}{\ell} = C_{\epsilon_2} \frac{u_{rms}^2}{T}, \tag{1.9}$$

where ℓ and T are the integral scales of length and time respectively, those being the largest such characteristic scales of the flow. The integral time scale is defined, in one manner, as follows:

$$T = \int_0^\infty \rho(\tau) d\tau, \tag{1.10}$$

where ρ is the autocorrelation coefficient of the fluctuating velocity component and τ is the time lag of the autocorrelation. In the context of biogenic turbulence, the magnitude of the dissipation rate is thought to be consistent (within an order of magnitude), over a wide range of species, within animal aggregations at a natural level of abundance [Huntley and Zhou, 2004]. However, controlled measurements of dissipation rate within realistic schools of fish are required to verify the accuracy of this claim. Additionally, such dissipation measurements may be directly compared with numerous measurements of background turbulence within various locations in the ocean, in order to further assess the role of biogenic turbulence in ocean dynamics.

It is important to note however that TKE is not dissipated at the large scales mentioned above; instead, there exists an energy cascade in which the TKE is transferred from the largest scales down through smaller and smaller eddies until reaching an approximate point at which the motions are dissipated by viscosity. These smallest scales, at which viscous dissipation occurs, are the Kolmogorov scales of length, time, and velocity respectively, uniquely defined by ratios of ν and ϵ as follows:

$$\eta \equiv (\nu^3/\epsilon)^{1/4} \qquad \tau \equiv (\nu/\epsilon)^{1/2} \qquad \upsilon \equiv (\nu\epsilon)^{1/4} \tag{1.11}$$

In practical applications, measurement devices must have resolutions finer than the Kolmogorov scales in order to fully resolve the turbulent motions. By measuring the dissipation

rate, and subsequently estimating the Kolmogorov scales, the suitability of various measurement techniques and instrument settings may be assessed (e.g. the sampling frequency of an ADV). Estimates of these scales may also provide insight into the structure of the turbulence under investigation, which in the case of biogenic turbulence is not well understood.

The energy cascade itself can be studied through the use of spectral analysis of the turbulence parameters, which can also be used to compare turbulence measurements to various idealized predictions. In the limit of infinite Re (or in real flows, $Re \gg 1$) and for homogeneous isotropic turbulence, the energy and velocity spectra have universal forms. Specifically, when plotted logarithmically, such spectra should decay with a slope of $-5/3$ in the inertial subrange [Pope, 2000]. Comparisons between the spectra of biogenic turbulence and idealized cases will contribute to the understanding of the homogeneity and isotropy of biogenic turbulence. This is a property that has been assumed in current literature [Katija, 2012], but has not been quantitatively analysed with regard to realistic animal aggregations.

Through the measurement and analysis of the characteristic scales, statistics, and spectra of biogenic turbulence as well as their comparison to idealized laboratory and oceanic flows, a more complete understanding of the structure and role of biogenic turbulence in the ocean may be developed.

1.3.2 Oceanic processes

To date, the description and understanding of many oceanic processes remains a complex and open problem. Specifically, there remains great uncertainty in the relative contributions of various individual phenomena, such as internal wave breaking, to the overall effects of large scale ocean circulation and local mixing. This uncertainty is the result of large gaps in available measurements, problems inherent to current measurement techniques, as well as the interconnectedness of and feedback systems within such processes.

Ferrari and Wunsch (2010) have attempted to concisely illustrate the complexities of ocean energy dynamics between sources (lunisolar tides, winds, and possible biomixing), sinks (various ocean layers), and energy dissipation mechanisms. In trying to find a balanced

system however, the authors acknowledge the large uncertainty in all estimates of fluxes and include only crude estimates of biological turbulence as a source of mixing while neglecting it as an energy dissipation mechanism. Clearly, to better inform this energy budget closure problem, more precise estimations of all sources and sinks are required, but particularly for the input from biogenic turbulence. Since it is the only direct source of TKE input to the upper/mid ocean, its effect on future closure models may be significant. Laurent and Simmons (2006) have estimated the total mixing power input required to balance this energy budget (or to sustain circulation) to be approximately 3 TW, with at least half required to be input at depths below the mesopelagic zone (an intermediate region, generally between depths of 200 to 1000 m below the surface). Ferrari and Wunsch (2009) find this to be a likely upper limit of the energy requirement, however, and suggest that 2 TW or slightly lower is a reasonable estimate for budget calculations. It remains unclear how this power is supplied, particularly in the abyssal ocean, where representative observations are sorely lacking. Biogenic turbulence remains a strong possible candidate contributing to this energy input, whose contribution could be assessed if the production of turbulence by small groups of animals can be observed and extrapolated to global population estimates. However, the impact of biogenic turbulence is complicated by factors such as the mixing efficiency of such fluid motions and the various biological parameters governing animal behaviour and distribution.

1.3.3 Biogenic turbulence

With the importance of the previously described processes in mind, and the continued uncertainty in the relative importance of contributors to the ocean energy budget, biogenic turbulence began to receive attention as a possible mechanism by which ocean stratification, mixing/circulation patterns, and energy dynamics could be affected. Biogenic turbulence research began with theoretical estimates, followed by oceanic and laboratory measurements, and, recently, numerical simulations.

Since the first mention, and subsequent dismissal, of the possible implications of biogenic turbulence [Munk, 1966], the impact of the biosphere on oceanic fluid dynamics only became a topic of fervent debate a little over a decade ago. The first theoretical estimates of the extent of biogenic turbulence were made by Huntley & Zhou (2004), by examining the amount of energy a fish would typically expend while swimming to overcome drag. Based on experimental observations of swimming mechanisms and exertion, the authors correlated the energy imparted to the surrounding water with fish Re and extrapolated these results to typically sized schools of a particular species. As all the energy imparted must eventually be dissipated by viscous effects, the rate of dissipation of TKE could be estimated from an overall energy budget. Their calculations suggested that not only do animal congregations exhibit dissipation rates of the same order of magnitude across a wide range of body lengths, but that biogenic dissipation rates are substantially higher than those typically observed as a result of significant wind and tidal forcing [Huntley and Zhou, 2004]. This study can be considered rigorous in that it took into consideration a wide range of available data on the biological parameters governing biogenic turbulence, such as abundance, aggregation size, variation of swimming speeds, and morphological effects on swimming efficiency. However, the conclusions lack the substantive evidence of direct measurements of biogenic turbulence and do not account for other behavioural and oceanographic parameters governing the results' applicability to ocean mixing.

Following Huntley & Zhou, and with complementary approaches, Dewar et al. (2006) attempted to estimate the total energy input into the ocean by the aquatic biosphere and its impact on the meridional overturning circulation (or MOC, a global network of ocean currents, encompassing both surface and deep layers, which contributes immensely to redistribution of salt and temperature). They instead considered the energy output from swimming of the entire biomass of the various ocean trophic levels as well as the fraction of net primary production which may be eventually transferred to turbulent kinetic energy or contribute to mixing at length scales above the Ozmidov scale. With attention to the turbulent mixing

budget described by Wunsch & Ferrari (2004) the authors conclude that a contribution to effective mixing on the order of 1 TW is not unreasonable. Again, the arguments presented were theoretical in nature, and the results do not provide adequate detail to be applied to ocean mixing and climate models. It is important to note that the trophic efficiency and biomass estimates for the mesopelagic region used in this study were likely gross underestimates [Irigoien et al., 2014]. Therefore, although estimates of photo-synthesizer biomass and TKE injection in the upper mixed layer made by Dewar et al. (2006) remain reasonable, the effect of biomixing on the MOC at depths below the typical extent of wind forcing are likely underestimated. This added error further clouds the waters surrounding how and to what extent biomixing influences the MOC at such depths, a process which Dewar et al. admittedly could shed little light on. The fact that these theoretical estimates, which placed substantial importance on the biospheres TKE input to the ocean energy budget and MOC, could indeed be underestimates within important sub-sea regions, warranted experimental studies on the ability of animals to effectively mix their marine environments.

The first measurements explicitly intended to measure biogenic turbulence were made by Kunze *et al.* (2006) in Saanich Inlet off the coast of British Columbia in Canada. The inlet waters were strongly stratified and shielded from strong tidal influences due to its geography, as well as being a known Pacific krill habitat. This combination provided an ideal location for *in situ* measurements, which were made using a ship-deployed microstructure profiler to estimate the dissipation rate of TKE, ϵ, and an echosounder to keep track of animal densities and migratory patterns. During periods of diel vertical migration of the krill, elevated levels of the dissipation rate were observed within the water column for approximately 10 - 15 minutes, particularly where the echosounder suggested the presence of the largest animals in dense aggregations. Although dissipation rates of $10^{-5} - 10^{-4}$ W kg^{-1} were measured (compared to typical background levels of $O(10^{-9})$ W kg^{-1}) there remained uncertainty in the exact abundance of the animals and whether the mixing efficiency within the aggregation

was high enough to overturn the stratification. Although lacking the control of a laboratory experiment, this study provides intriguing results suggesting the possible importance of biogenic turbulence associated with vertically migrating species.

Similar to Kunze et al. (2006), Gregg and Horne (2008) measured the dissipation rate and diapycnal diffusivity using a microstructure profiler in what appeared to be several aggregations of small fish in Monterey Bay. Although elevated levels of dissipation rate, on the same order of magnitude as those of Kunze et al. (2006) were observed within the aggregation, no substantial change in diapycnal diffusivity was detected and the mixing efficiency was 0.0022, almost a factor of one hundred lower than that outside the aggregation. The authors were cautious in their conclusions however, noting that the composition of the aggregations was ill-defined and encounters with the animals were intermittent and left to chance. Although intriguing, these results further underscore the need for well defined experiments which can provide representative data describing this problem.

Adding to the complexity of the biogenic turbulence question, Katija and Dabiri (2009) suggested a previously overlooked mechanism by which aquatic animals, particularly vertically migrating species, could further affect ocean mixing. It was suggested that Darwin drift could substantially add to previous estimates of biogenic mixing due to the fact that this mechanism is enhanced by viscosity (or at low Re) [Darwin, 1953]. Darwin drift is the mechanism by which a volume of fluid proportional in size to the volume of a submerged object is forced to drift with the motion of that object. By injecting dye into the path of swimming jellyfish and recording the interaction via underwater camera equipment [Katija and Dabiri, 2008], measurements of the fluid drift induced by isolated animals were made. From these results, as well as simple computer simulations to corroborate the experimental results, the dissipation rate resulting solely from induced drift was estimated to be on the order of $10^{-5} - 10^{-4}$ W kg^{-1}. However, although dissipation rates were substantial, the measurements were only made on isolated animals, thus excluding possibly enhanced mixing due to wake interaction in dense aggregations. Again, the results were intriguing, but cannot

be considered representative due to the fact that Darwin drift is dependant on morphology and could not be extrapolated to whole aggregations, particularly those of different species.

Lorke and Probst (2010) also made microstructure measurements using a bottom mounted profiler in a freshwater lake. The profiler was placed off of a pier around which perch were observed schooling, however, occurrences of fish abundance substantial enough to have a measurable effect on the dissipation rate were rare. The high intermittency of these results suggested that biomixing is likely not important in such shallow waters with low abundance, non-migrating species. Rousseau et al. (2010) attempted to rule out other situations in which biomixing was thought to be possibly significant, by revisiting the Saanich Inlet site [Kunze et al., 2006] as well as another established ocean research site in the Canadian Pacific Subarctic (Site P). At Saanich Inlet, the bursts of high-intensity turbulence associated with elevated dissipation rates were found to be extremely rare, comprising only four percent of the recorded krill activity. At Site P, where animal aggregations are considerably less dense but comprised of individuals with Re of 1000, similar turbulence bursts were also rare. It has thus been suggested that mixing at these sites is too inefficient to significantly disturb the established stratification, or is only at a level comparable to other processes. Again, however, these measurements suffer from the inconsistency of a wide range of parameters impacting ocean-based measurements (unclear structure and composition of aggregation, complex animal behaviour, influence of background flow on animals, etc.).

The first laboratory-based measurements of biogenic turbulence were made by Noss and Lorke (2014) within a migrating swarm of zooplankton (*Daphnia magna*). By controlling animal movements using LED light panels, zooplankton migration was induced throughout a stratified water column, in which laser-induced fluorescence (LIF) was used to measure the concentration of a fluorescent dye (Rhodamine 6G) and thereby estimate the diffusivity within wakes of individual animals and broadly throughout the swarm. Although *Daphnia* are known to produce relatively large, energetic wakes and drift volumes

[Wickramarathna et al., 2014], including in the presence of potentially toxic substances employed as tracers [Noss et al., 2013], diffusivities were found to be comparable to that of salt. The lack of elevated diffusivities suggests that even the bulk motion of such small, low Re, animals cannot substantially overturn stratification typical of lakes and oceans. These results are consistent with the predictions of Kunze (2011), however they can only be considered a limiting case for animals of this particular size, morphology, and Re.

Using a laser guidance system, Wilhelmus and Dabiri (2014) were able to induce diel vertical migration of the plankton *Artemia salina* (commonly referred to as brine shrimp) in a more controlled fashion as compared to the LED technique of Noss and Lorke (2014). During the vertical migration, large scale fluid motions were observed using particle image velocimetry (PIV). Although these experiments were conducted in an unstratified water column, and thus do not provide insight into mixing efficiency or estimates of induced diffusivity, a Kelvin-Helmholtz instability and fluid structures comparable to the aggregation size resulting from the bulk movement of the animals were observed. This finding suggests that animal aggregations as a whole may influence their surroundings based on collective behaviour and may be able to affect stratification and mixing depending on abundance and the size of individual animals. Whether these fluid motions are representative of all vertically migratory species, how they are affected by stratification, and their interaction with fluid drift and other processes remains unclear. However, the fact that the energetics and mechanics of aggregations are seemingly more important that those of individuals has been made clear by both this study and that of Noss and Lorke (2014).

Controlled turbulence measurements within a school of juvenile Atlantic salmon *Salmo salar*, the largest Re animal investigated in a controlled environment so far, have been made by Plew et al. (2015). Motivated by the importance of oxygen dispersion in aquaculture enclosures for fin fish, measurements of oxygen concentration and water velocity were made in a circular holding tank with an inflow current with and without fish present. Velocity measurements were made using an ADV and revealed that biogenic turbulence reduced the

mean water velocity (compared to the case without fish present) by 15-57% depending on the abundance in the tank. Additionally, estimates of TKE and its ϵ were substantially higher in the presence of fish, and the transport of dissolved oxygen was enhanced. This result suggests that animals of high enough Re in normal levels of abundance can significantly impact the transport of nutrients and dissolved gasses, processes which could possibly be important for smaller oxygen and nutrient dependent species within the same biome. It remains to be seen, however, what the lower Re limit is for fin fish to inject energy and affect mixing at a substantial rate, and whether or not the bulk motion of fish schools similar to those of Atlantic salmon can have further implications for ocean mixing.

In an attempt to address scepticism regarding the importance of drift to biogenic mixing [Kunze, 2011] and its dependence on animal morphology [Katija and Dabiri, 2009], Katija (2015) made both laboratory experiments and numerical simulations in which the drift volume was measured. PIV measurements were made in the flow around swimming jellyfish (*Phyllorhiza* sp.) with and without their oral arms removed to map the induced velocity field for two morphologies. This velocity data was used in numerical simulations to estimate the corresponding drift volume and was compared to that obtained using the velocity field around a sphere in potential or Stokes flow. This is in contrast to methods in which swimming animals are modelled with force dipoles or towed bodies [Subramanian, 2010] whose resulting estimates for drift volume have been questioned [Ardekani and Stocker, 2010]. It was found that the sphere in potential flow resulted in a substantial underestimate of the jellyfish drift volume while the Stokes flow simulation resulted in a gross overestimation. Additionally, the animal with oral arms was more effective in inducing vertical fluid transport than those without such appendages. These results highlight not only the importance of considering drift when estimating biogenic mixing but also the difficulty in scaling or applying the turbulence characteristics of specific animals to others with even slight differences in morphology. This work underlines the need for more and diverse laboratory data (with regard to species and morphology) for the purpose of large scale modelling of the impacts of biogenic turbulence.

Wang and Ardekani (2015) performed a large set of numerical simulations in order to better evaluate possible contributions to ocean mixing due to low-Reynolds number swimmers. This work tested the prediction that such swimmers cannot generate mixing more significant than that occurring due to molecular diffusion [Kunze, 2011] and correlated turbulent mixing parameters with Reynolds number. The simulations were performed by resolving a flow field containing model swimmers, both allowed to move freely throughout the domain and constrained to vertical motion, in both turbulent and quiescent fluid backgrounds, complementing previous experiments with vertically migrating species [Noss and Lorke, 2014, Wilhelmus and Dabiri, 2014]. While the simulation results agreed with results showing that organisms with $Re < 1$ are not able to induce significant mixing, there was found to be a clear trend of increasing diapycnal eddy diffusivity with increasing swimmer Re over the sample range of $Re \sim O(0.1 - 100)$. Additionally, fluid transport was enhanced both when the swimmers were constrained to vertical motion and in the presence of background turbulence and most importantly was comparable to that due to internal wave breaking. These results further stress the importance of correlating biogenic turbulence parameters with animal Re as well as the importance of behavioural parameters when investigating biogenic turbulence in both laboratory and numerical investigations. Furthermore, the Re dependency suggests that future experiments should not only encompass a similar range, but extend beyond the maximum value of 100 to better represent the diversity of animal size and behaviour at mesopelagic depths.

Hooper et al. (2016) have made simultaneous measurements of acoustic backscatter and turbulence statistics within a surface scattering layer and a deep scattering layer comprised mainly of Nekton. Most importantly, the deep scattering layer measurements were made below the euphotic zone, both during instances of diel vertical migration and while the deep scattering layer was stationary. These shipboard experiments were conducted across a clover-shaped region off the coast of the Bahamas in an area known as the tongue of the

ocean. While the results are representative of a larger area than previous studies, the investigation was nonetheless relatively localized, with sampling times and locations also limited by weather and vessel availability/priorities. Nonetheless, the elevated levels of dissipation rate within the surface scattering layer and deep scattering layer during diel vertical migration ($O(10^{-7})$ and $O(10^{-8})$ W kg^{-1}, respectively, compared to background levels of $O(10^{-10})$ W kg^{-1}) provide evidence that TKE transferred to the ocean by preying and migrating nekton may be significant. As with other earlier field measurements however, the mixing efficiency has not been investigated nor has the structure and composition of the animal aggregation been accurately defined. Moreover, there is substantial variability between the 18 data sets presented in this work, with no precise explanation for the reasons thereof, whether physical, biological or a combination of the two. However, in addition to reinforcing the need for more accurately observable experiments on biogenic turbulence, the results seem to demonstrate a relationship between volume backscatter and dissipation rate, which can best be verified through an investigation on the effect of abundance on biogenic turbulence production.

Dean et al. (2016) attempted to shed light on the discrepancy between the results of Kunze et al. (2006) and Rouseau et al. (2010) and the effects of biomixing on pollutant dispersion by investigating the turbulence generated by zooplankton in the Straits of Florida undergoing diel vertical migration. Additionally, numerical simulations were performed to complement the experiments and further isolate the factors contributing to the variability of *in-situ* observations. Using a bottom mounted acoustic Doppler current profiler, swarms of sound scatterers were identified and velocity measurements were recorded over an eleven-month period. It was found that during instances of diel vertical migration, the mean velocity of the local ocean current was slightly suppressed and that this result was consistent with the accompanying numerical simulations. The simulations also demonstrated the effect of animal abundance on biogenic turbulence production with estimates of dissipation rate up to $O(10^{-6})$ W kg^{-1} for $A = 10000$ organisms/m^3 as opposed to ($\sim O(10^{-7})$ W kg^{-1}) for $A = 1000$ organisms/m^3. This range could explain the variation in Saanich inlet data, which

had no accompanying estimates for the abundance levels. Additionally, the effects of the biogenic turbulence on the mean flow are consistent with both the numerical simulations and the observations of Plew et al. (2015). Though these results are intriguing and clearly build upon earlier work, the experiments themselves were in an environment no more controlled or well-defined than those in Saanich inlet and the swimmer model used in the simulations was not as well refined as that used by Wang and Ardekani (2015). Despite these drawbacks, the work clearly emphasizes the need for controlled laboratory experiments which can vary parameters such as abundance to further benchmark the contribution of biogenic turbulence to ocean ecosystems.

Finally, Tanaka et al. (2017) have directly investigated dissipation rates within schools of Japanese sardines, one of the species considered in the hypotheses of Huntley and Zhou (2004). In comparison to previous experiments, these measurements were performed in the fairly well-controlled environment of a commercial aquarium, however, similar to Plew et al. (2015) the tank contained measurable background turbulence. The behaviour of the school of sardines was also heavily influenced by the presence of other species of animals scattered throughout the aquarium, including natural predators which induced avoidance behaviour, as well as instances of feeding, during which the sardines exhibited predation behaviour. The resulting measurements, made using a free-ascending microstructure profiler, demonstrated dissipation rates $O(10^{-4})$ W kg^{-1}, compared to background levels $O(10^{-6})$ W kg^{-1} outside the school of fish. These values are both above those predicted by Huntley and Zhou (2004) as well as background turbulence in the ocean, and also demonstrate behavioural dependencies, based on video observations of the school during data sampling. However, whether these trends can be extended to other, less energetic and complex, behaviours is unclear, and furthers the case for baseline measurements of biogenic turbulence with as few behavioural influences as possible.

In summary, the state of the art surrounding biogenic turbulence lacks both a clear consensus regarding small-scale and global impacts of such fluid motions, as well as a clear

understanding of the fundamental relationships between biological parameters and the structure of turbulence generated by various portions of the biosphere. The most logical steps toward a firm foundation on which to draw conclusions regarding the importance and influence of biogenic turbulence, are rigorous yet simple and controlled laboratory studies of various animal aggregations and the fluid dynamics that they collectively induce.

1.3.4 Acoustic Doppler velocimetry

Acoustic Doppler velocimetry has played an essential role in both fundamental and environmental fluid mechanics research over the last five decades. ADVs are rugged instruments that have been adapted for both laboratory and field measurements in a wide range of settings, for example [Brand et al., 2016] and [Liljebladh and Thomasson, 2001]. ADVs are bi-static SONAR instruments which transmit pairs of pulsed ultrasonic signals and detect the corresponding reflections from small suspended particles in the fluid environment. By recording the difference in frequency between each pulse and measuring the phase lag between transmitted and received pulses, the velocity of the particle, and, by extension, the fluid, may be inferred via the Doppler effect formula. The general performance of ADVs for turbulence measurements has been well-documented [García et al., 2005] and in particular, noise in ADV measurements has been quantified in various studies and can be addressed through several correction methods [Khorsandi et al., 2012]. Notably, ADVs with transducer arms mounted at an angle to the probe head, such as the Nortek Vectrinos used in this work, tend to have substantially higher levels of signal noise in the horizontal components of the measured velocity (denoted the x and y-beams of the ADV, as opposed the vertical z-beam which is aligned with the probe head). One other important characteristic of down-looking ADV probes is the fact that sound transmissions induce a mean velocity along the probe axis (called acoustic streaming), which may affect the flow under investigation [Pointdexter et al., 2010]. The two instruments used in this study were the four-beam, 10 MHz Nortek Vectrino ADV, with a down-looking, flexible cable probe (with a 1 m cable) and Nortek Vectrino Profiler profiling ADV, with a down-looking fixed stem probe, as shown in figure 1–1. Both instruments are

pulse-coherent Doppler processing devices, which record velocity in three orthogonal directions [Nortek, 2004, Nortek, 2012], and can estimate spectral moments through pulse-pair or autocovariance estimation [Lhermitte and Serafin, 1984]. For the sake of clarity, the standard Vectrino will henceforth be referred to as the Single-point Vectrino to differentiate from the Vectrino Profiler, with specific details of their use provided in section 2.2.

Figure 1–1: Nortek Vectrinos with down-looking, fixed-stem and flexible cable probes, respectively [Nortek, 2013].

The Single-point Vectrino estimates velocity at a single point, by averaging measurements made within an approximately cylindrical sampling volume located roughly 5 cm below the probe head. The dimensions of the sampling volume and transmission power of the instrument are both related and user-selected (with larger power levels allowing larger dimensions, but inducing more intense acoustic streaming). The Single-point Vectrino can also be configured with a range of pre-calibrated velocity ranges, which, along with power levels, have an effect on signal quality parameters such as signal-to-noise ratio (SNR), signal correlation percentage (correlation), and signal amplitude (in dB). These parameters can be recorded in tandem with velocity at a maximum sampling rate of 25 Hz.

The Vectrino Profiler shares the same electronics housing and other structural components with the older, standard Single-point Vectrino, but features more advanced and alternatively-configured electronics, which allow for the measurement of velocity along a vertical profile (that is, along the same axis as the probe head). The top of the profile is offset

approximately 40 mm from the probe, with an adjustable height ranging from 10-30 mm, and is divided into individual sampling volumes, or bins, of 1-4 mm in height. The signal quality however, similarly affected by power and velocity range settings, but measured at every bin, is not constant over the profile. The region of highest quality is generally located around 50 mm from the probe head and is referred to as the sweet spot. The Vectrino Profiler also allows the sampling frequency to be selected from 25-100 Hz. Finally, it should be noted that the Vectrino Profiler is a relatively new instrument, which, although extremely similar to the older, standard Single-point Vectrino, has not been extensively validated. While the two instruments have been compared in turbulent flows [Zedel and Hay, 2011, Craig et al., 2011], the ability of the instruments to precisely measure quantities such as dissipation rate, or the downstream evolution of flow variables in a turbulent jet have not been documented publicly. Regardless of noise, acoustic streaming, and often limited resolution, ADVs continue to be indispensable for the study of environmental fluid dynamics, and, upon further validation, promising tools in the characterization of biogenic turbulence.

1.4 Document outline

The remainder of the thesis is organized as follows. Chapter 2 describes the methodology of the biogenic turbulence experiments, including the species used, compliance with animal ethics protocols, the experimental apparatus and instrument parameters, and data analysis procedures pertinent to biogenic turbulence measurements. Chapter 3 outlines experiments made in a turbulent jet, to compare the performance of the two ADVs used throughout this study, as well as the corresponding results. Chapter 4 presents the results of the experiments performed with fish and their interpretation, including comparisons with previous biogenic and representative oceanic turbulence data. Chapter 5 highlights the sources of error and uncertainty associated with the results presented, and how their interpretation is affected. Finally, Chapter 6 presents conclusions as well as suggestions for future work related to this study.

CHAPTER 2
Experimental methods

The measurements of biogenic turbulence described in this thesis were made in the Environmental Hydraulics Laboratory of the Department of Civil Engineering and Applied Mechanics at McGill University. The procedures related to animal care and experimentation were conducted with prior approval of the University Animal Care Committee (UACC) as detailed in Protocol #2014-7505. The details of the animals and their enclosures, instrumentation, experiments, and data analysis are described below.

2.1 Animals and animal housing

Two species of tetra fish were used for the experiments. The first, a population of 5 male and 45 female Congo tetras (*Phenacogrammus interruptus*), ranging in size from approximately $5 - 8$ cm in length, which were housed in $91 \times 30 \times 45$ cm glass aquarium. Second, a population of 50 smaller neon tetras (*Paracheirodon innesi*), of undetermined gender, approximately $3 - 4$ cm in length, which were housed in a $60 \times 35 \times 31$ cm glass aquarium, and shown, along with the Congo tetras, in figure 2–1. Tetras were selected as alternatives to the various Clupeiforme species (herring, sardine, anchovy) examined by Huntley and Zhou (2004), as they are comparatively inexpensive and readily available, hardy and simple to maintain, and, importantly, form shoals and/or schools of similar abundance to small Clupieformes, as well as other fish and invertebrates.

When not in experimental configurations, the aquariums were equipped with an appropriate amount of environmental enrichment (3-5 cm gravel bed, stones, driftwood, plants, etc.) and monitored in accordance with McGill University's Aquatic Animal Standard Operating Procedure (SOP) and animal care guidelines [Gourdon, 2009]. Additionally, water quality was monitored and adjusted daily to consistently ensure that concentrations of ammonia and nitrite were below 0.25 ppm, concentration of nitrate was below 40 ppm, and the

(a) Congo tetras

(b) neon tetras

Figure 2–1: The aquaria housing two species of fish used in the experimental procedures, shown in non-experimental configurations.

pH of the water was approximately 6.7. Water changes were performed as required, generally 15% per day, using filtered and treated water contained in reservoirs below the tanks. The reservoirs were replenished weekly using water treated with a Jacuzzi® Laser 192 sand filter, Pentair Logix™764 softener (using Windsor® System Saver® II salts) and API Proper pH® 6.5. Before being added to the aquariums, this water was allowed to stand for 24 hours to allow for the evaporation of any residual dissolved chlorine. Both aquariums were heated

with Eheim Jäger TruTemp® series submersible heaters to maintain a water temperature between 26 and 28 ℃. Additionally, the aquariums were continuously filtered with Marineland Penguin® Bio-Wheel® series filters. Timed lighting and automated feeders were used to ensure consistent amounts of 'daylight' and a structured feeding schedule. Specifically, a 36" long, 38 W fluorescent aquarium lamp suspended above the Congo Tetra tank and a 40 W desk lamp placed above the neon tetra tank provided illumination between 6:00 AM and 6:00 PM. Meanwhile, an Eheim Everyday Fish Feeder™ dispensed a mixture of Tetramin® Tropical Crisps and TetraColour® Spirulina flakes at 9:00 AM and 5:00 PM. Given the behavioural similarity to various species considered as biogenic turbulence-producing candidates and the hardiness of the species, Congo and neon tetras were an appropriate and effective test species for lab-based measurements of biogenic turbulence.

2.2 Experimental apparatus and procedure

The experiments were performed at fixed times of day and with a standardized procedure, with measurements being made within the two schools of fish, over a range of abundance levels, using predominately the Single-point Vectrino, described in the previous chapter. The experimental procedures as detailed below were classified as B-Level invasiveness in the animal use protocol, and no long-term adverse effects on animal health were anticipated or observed as a result of the experiments.

All experiments were performed within the animal housing enclosures after being converted into what will be referred to as the experimental configuration. The procedure was conducted such that each time series began $6 - 6.5$ hours after 'sunrise' (referring to the timed aquarium lighting turning on at 6:00 AM every morning) and $3 - 3.5$ hours after the most recent feeding of the fish. The consistency of experiment times served to eliminate any behavioural bias, which could be attributed to variations in hunger or fatigue. Moreover, the delay between feeding and measurements provided ample time for fish predation behaviour (associated with high swimming speeds, complex trajectories, and interaction between animals) and the mating behaviour which often followed, to normalize. First, beginning at

approximately 11:45 AM, all filters, heaters and environmental enrichment features, except for the aquarium gravel, were removed from the tanks with as little disturbance as possible, so as to avoid inducing stress on and panicked behaviour of the fish that may affect results. Attention was also paid to the placement of any inanimate objects near the tanks which could influence the behaviour or orientation of the school. Plexiglas dividers were then inserted into the tank to constrain the fish to one of six predetermined volumes (as shown in figures 2–3 and 2–4), thereby controlling the minimum abundance of the aggregation. The dividers were cut from a Plexiglas sheet as shown in figure 2–2 allowing them to hang from the plastic trim of the aquariums by the upper protrusions, but long enough to be set into the aquarium gravel. The flaps of plastic screening along the vertical edges closed the gap between the divider and glass sides of the aquarium, preventing any fish from escaping the experimental enclosure.

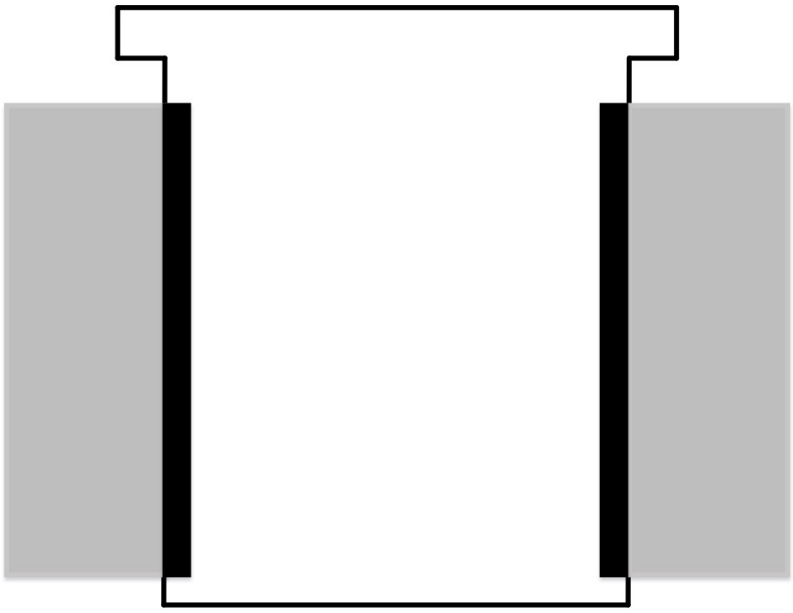

Figure 2–2: Schematic of tank divider (not to scale).

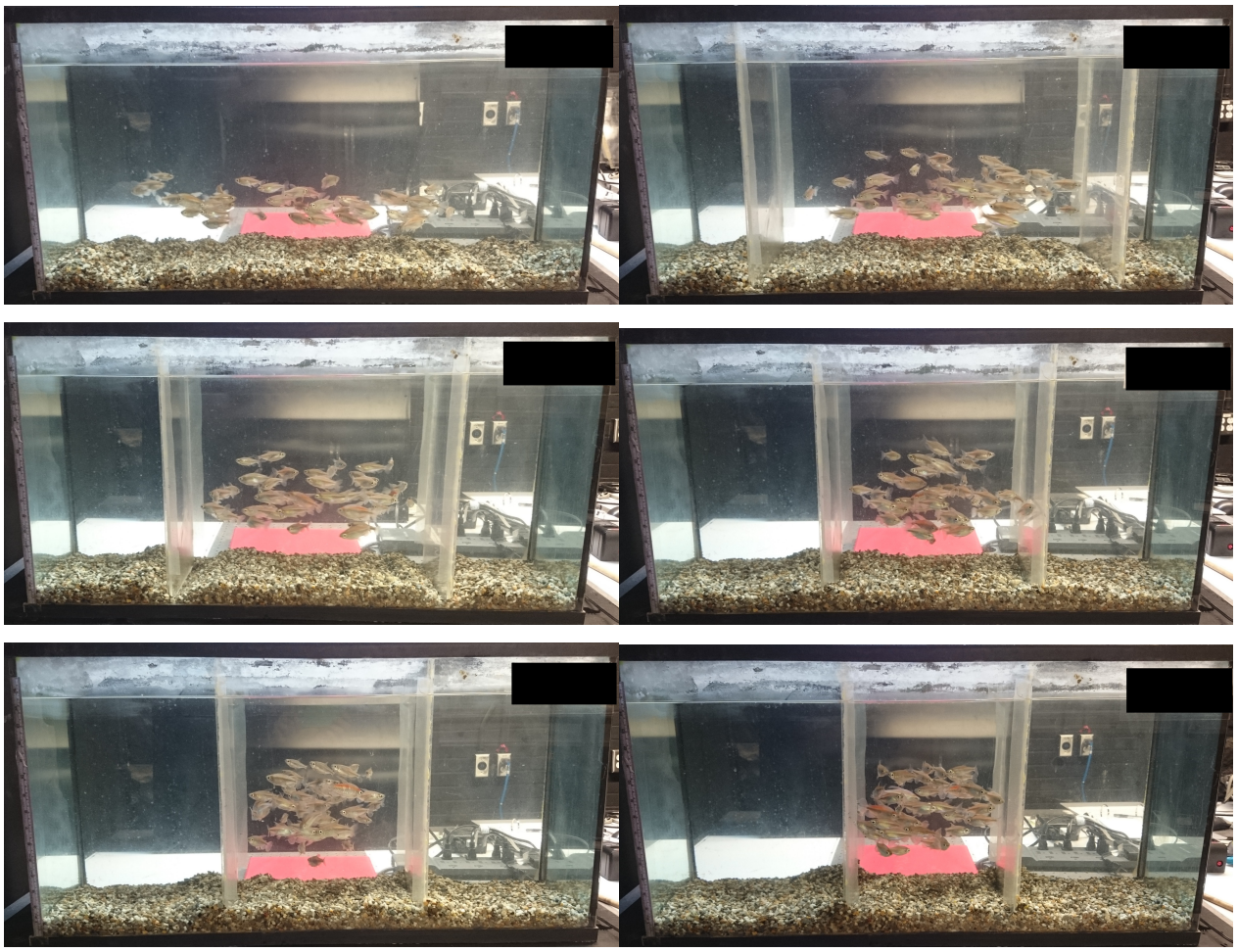

Figure 2–3: Six enclosure volumes used for Congo tetra experiments, corresponding to minimum abundances of 500, 750, 1000, 1250, 1500, and 1750 animals/m^3.

Figure 2–4: Six enclosure volumes used for neon tetra experiments, corresponding to minimum abundances of 2250 and 2500 animals/m^3.

The ranges of abundance were chosen to reflect that which would be observed in a natural environment for similar sized, schooling fish. However, the lower limit of the Congo tetra

abundance range was defined by the size of the tank, whereas, at the upper limit, any further decrease in the volume of the experimental enclosure was found to significantly increase the probability of panicked behaviour and overall stress on the fish. Additionally, the lower neon tetra abundance limit was determined by the observation that at lower abundances, the disturbances produced by the fish were both unlikely to be in the vicinity of the ADV sampling volume or produced a highly intermittent turbulent velocity signal. The upper limit however, was governed by the minimum distance between the Plexiglas divider and ADV, such that the signal was not adversely affected by wall echoes ($\sim$ 5 cm).

Once again, two ADVs were use for biogenic turbulence measurements, however, the Vectrino Profiler, which was used on loan from the Institut national de la recherche scientifique - Eau Terre Environnement (INRS-ETE), and was only available for preliminary measurements with the Congo tetras and the validation experiments described in the next chapter. The Vectrino Profiler was configured with a sampling rate of 100 Hz, a power level of High, and sampled over a vertical profile of 25 sample bins, each of 1 mm in height. Within the 35 mm profile, the so called sweet spot of the signal was found to be between the 8th and 13th bins. On the other hand, the Single-point Vectrino was configured with a 25 Hz sampling rate, a power level of High, and 2.4 mm diameter by 9.1 mm height sampling volume. The velocity range was set to 10 cm s^{-1} for Congo tetra experiments and 3 cm s^{-1} for neon tetras.

With the tank dividers in place, one of three mounting stands (shown in figure 2–5) was placed atop the aquarium, after which the corresponding ADV probe was inserted into the water, secured to the stand and levelled. The electronics housing of the Vectrino Profiler was held in a single orientation by padded hose clamps, which were affixed to a flat wooden block. The block was bolted to a steel frame which was fit over the top edges of the tank. For the Single-point Vectrino, however, the probe was held by a test tube clamp, which was affixed to vertical shaft, bolted to an aluminium bracket which ran across the top of the tank. The bracket was built to the standard tank width and was therefore held firmly in place by the slight outward bowing of the tank edges due to hydrostatic water pressure. The

electronics housing of the Single-point Vectrino was placed on the table-top, as far from the enclosure volume as the probe cable would allow and excess length of data transmission cable was coiled tightly on the tabletop to reduce signal noise. In the vertical configurations of Figure 2–5) a) and b), the ADV probe heads were submerged approximately $3-5$ cm below the surface of the water, thereby allowing adequate distance between the sampling volume and the tank bottom (at least 15 cm) to minimize bottom echo noise. Moreover, the probes were horizontally centred in the enclosure to minimize noise from wall echoes. The vertical orientation was used for measurements over the full range of abundance, as it allowed for a greater range of enclosure volumes and comprised fewer physical submerged components

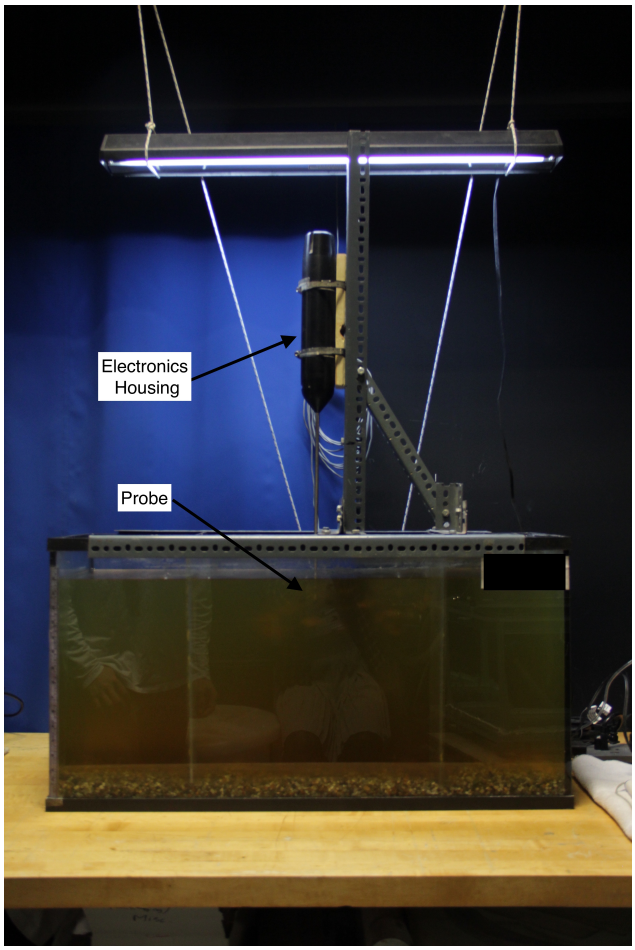

(a) Vectrino Profiler in Congo tetra tank, seeded with algae, and showing overhead aquarium lamp.

(b) Vertically oriented Vectrino in the unseeded neon tetra tank.

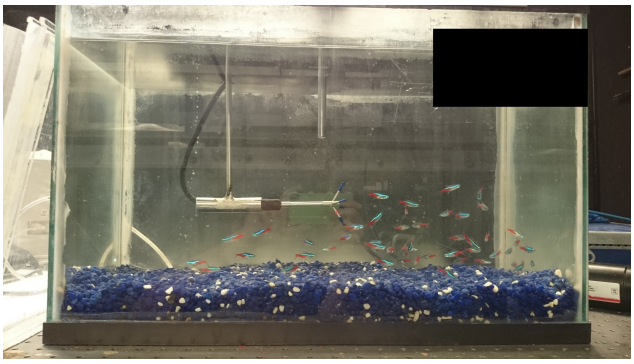

(c) Horizontally oriented Vectrino in the unseeded neon tetra tank.

Figure 2–5: Three ADV mounting arrangements used in the experiments.

which could affect fish behaviour and school orientation. The horizontal orientation of the Single-point Vectrino probe (Figure 2–5 c) allowed for the characterization of the isotropy of the biogenic turbulence, by comparing two orthogonal components of velocity, measured with the low-noise z-beam of the ADV.

As the aquariums were cleaned daily and filtered continuously, the water generally contained an insufficient amount of suspended particles to facilitate accurate ADV measurements. Thus, the water was seeded with concentrated inert algae, which, while clouding the aquarium water and raising its pH above 7.2 over the course of each experiment, did not noticeably affect fish health or behaviour. Specifically, the algae *Thalassiosira weissflogii*, a diatom of cell dimensions $6 - 20$ μm $\times$ $8 - 15$ μm, was obtained from Reed Mariculture (Instant Algae® TW 1200). This species was found to provide adequate signal quality in simple ADV tests, and was subsequently used for all experiments with the fish. In each experiment, after the ADV had been installed, algae concentrate ($\sim$120 mL diluted in a 500 mL graduated cylinder for the larger tank, and $\sim$70 mL for the smaller tank) was gradually added to the entire tank and gently stirred to uniformly seed the water. After the algae was added, the water was allowed to stand for approximately 5 minutes to allow for any stirring-induced disturbances to dissipate before recording any data. This delay also allowed the fish behaviour to normalize, so as to not be influenced by changes in the aquariums configuration, and to acclimate to the change in visibility and pH due to the addition of the algae. Following this standing period, the ADV was activated and allowed to record time series of velocity, signal-to-noise ratio, signal amplitude, and signal correlation percentage for $20 - 25$ minutes, depending on the stability of the signal quality and/or signs of fish stress. During data recording, qualitative observations were made regarding the general swimming speed and instances of escape speed manoeuvres, structure and orientation of the school, as well as any spatial or directional biases that could be noted. Movements around the tank were limited or made slowly, so as to minimize any influence on the behaviour of the fish. After an experiment was completed, the ADV and tank dividers were promptly removed and

a 15% water change was performed before replacing filters, heaters, etc. The majority of the algae was completely removed by the filter within 24 hours, after which the aquarium's pH was readjusted to approximately 6.7. Experiments were never run more than two days in a row, so as to allow the tank to be kept consistently clean and with adequate water quality, as well as to mitigate any compounding of stress on the animals (and the corresponding consequences to repeatability) caused by the experimental procedures. Measurements at each different abundance were made successively (i.e. 500,750,...1750,500,... animals/m^3) in an effort to balance out the effects of any animal growth over all abundances. In general, three experiments were required at each abundance to achieve convergence of the results of interest, however, additional experiments were performed at 1250 animals/m^3 to investigate behavioural consistency over a greater number of measurements. In summary, through the performance of behaviourally consistent experiments, over a range of abundances, and with multiple ADVs and probe orientations, the structure and dynamics of biogenic turbulence could be thoroughly investigated within schools of two fish species. The interpretation of the resulting data, however, required particular care to accurately quantify the turbulence generated by these animals.

2.3 Data processing

In analysing the ADV time series data obtained by the aforementioned procedure, careful consideration was given to signal filtering, modifying standard numerical procedures to accommodate filtered time series, and the estimation of the dissipation rate. Specifically, data points which corresponded to the presence of a fish within the sampling volume of an ADV had to be removed from the data sets, which led to discontinuities of significant length and frequency throughout the data. These discontinuities complicated the calculation of turbulent spectra and statistical quantities such as autocorrelations. Additionally, due to the different capabilities of each ADV, two methods of estimating the dissipation rate were employed, both of which were affected by the 'gappy' tendency of the data. The majority of the data analysis was performed using custom MATLAB programs.

In general, having a collection of relatively large solid objects, or in this case, animals, in close proximity to the sampling volume of an ADV can be expected to result in added noise within the data. However, the presence of fish in the ADV sampling volume was not found to produce erroneous spikes of velocity readings in the same manner as a strong bottom echo would, for a probe in close proximity to a solid wall. Nonetheless, a fish swimming through the sampling volume or positioned against or immediately below a transducer arm was found to produce positive and negative spikes in signal amplitude, respectively, as well as significant decreases in SNR and correlation. These effects were noted by simply watching the data recording interface and fish locations at the same time, as well as investigated using towed fishing lures, as described in previous work [Camozzi, 2015]. Given the ability of both ADVs to record these signal quality parameters simultaneously with velocity, data points with at least one signal quality parameter having a value below the threshold, as suggested by the ADV operating guidelines, were excised from the time series and replaced with NaN in MATLAB. In the case of the Vectrino, the minimum amplitude, correlation, and SNR were taken to be 80 counts, 80%, and 15 dB, respectively, while the minimum amplitude for Vectrino Profiler data was -55 dB, as it is recorded in an inherently different fashion than that utilized by the Single-point Vectrino. The gaps left between valid data points were not interpolated across, as this would have been impractical and inaccurate given the length of some gaps (in some cases several seconds) and the frequency of inadmissible points (as much as half of all samples in an experiment, in many cases). Although straightforward and relatively simple to implement, the impact of this filtering method on the data analysis and experimental uncertainty required further consideration.

This filtering method was not shown to have a significant impact on mean and RMS statistics, as discussed in the following chapter. However, the resulting gappy data was particularly complicating to the calculation of autocorrelations and velocity spectra, both of which required customized MATLAB programs to handle the modified time series. The programs identified segments of uninterrupted data points with a length greater than some

user-specified threshold (a power of 2, for the spectra code), then made subsequent calculations on each permissible segment, and finally averaged the collection of individual results. In taking this approach, the temporal extent of the autocorrelation and its convergence at high lag-times was severely limited, while the frequency range of velocity spectra was similarly limited. Although further analyses such as the estimation of integral time scales were still possible, the effects of the gappy data on uncertainty and error propagation are non-negligible and discussed in Chapter 4.

Using measurements of RMS velocities and estimates of the integral time scale, the dissipation rate could be estimated, on an order of magnitude basis, using the single point Vectrino data according to equation 1.9. However, in the present results, the autocorrelation curve was integrated only to the first point at which it crossed the x-axis. Alternatively, the vertical profile of velocity data obtained via the Vectrino Profiler was used to estimate velocity gradients and thereby approximate the dissipation rate through equation 1.8. Velocity gradients were estimated using 2nd and 4th order, centred finite differences, depending on the amount of data available (4th order differences do not converge as quickly, because of the lower probability of having 5 consecutive bins uncontaminated by fish, compared to 2nd differences). The equation for the second order difference at the i$^{\text{th}}$ bin of the vertical velocity profile is [Burden and Faires, 2011]:

$$\left(\frac{\partial w}{\partial z}\right)_i \approx \frac{w_{i+1} - w_{i-1}}{2h_z}, \tag{2.1}$$

where h_z is the bin size (1 mm). Although the former method may not have been as accurate as the more direct estimates utilizing the velocity profiles, it was nonetheless useful due to the limited availability of the Vectrino Profiler. However, whenever possible, the results of both methods were compared for consistency, with both biogenic turbulence data and that obtained in a separate validation study based on measurements within a turbulent jet.

CHAPTER 3
Validation of ADV performance in a turbulent jet

The use of the Vectrino Profiler for lab-based turbulence measurements has not been well documented. Specifically, the performance of the Vectrino and Vectrino Profiler have not been directly compared, nor has the ability of either instrument to accurately estimate the dissipation rate been thoroughly examined. In an effort to characterize the performance of both ADVs, turbulence measurements were made, with both instruments, along the centreline of a turbulent jet at four downstream locations. The measurements made by the two devices were then compared to each other, as well as with the established data on turbulent jets. The detailed procedure of these measurements, as well as the presentation and interpretation of the results, are described below.

3.1 Turbulent jet apparatus and procedure

The experiments were conducted in a $3 \times 0.7 \times 0.8$ m^3 tow tank with the jet fixed near one end, and centred in the other two dimensions of the tank. The tank was also equipped with an overflow, located at the end opposite the jet, to maintain a constant water level in the tank. The tow tank overflow drained into a ground-level reservoir which supplied an approximately 400 L constant head tank, located $\sim$3.4 m above the jet exit, via a 1/2 hp MARCH® (Model DP-6T-MD) centrifugal pump. The constant head tank was also fitted with an overflow, feeding back into the reservoir. The discharge of the 15 mm diameter jet was controlled by an adjustable Dwyer® Rate-Master® flowmeter, mounted on the side of the tow tank, between the constant head tank and jet pipe structure, to maintain a jet Reynolds number of approximately 12 000. A schematic of the apparatus is shown in figure 3–1 (note the reference axes at the jet exit).

The Vectrino ADV probe was oriented horizontally on a bracket and could be moved in the y and z directions, while the electronics housing of the Vectrino Profiler was fixed to a two

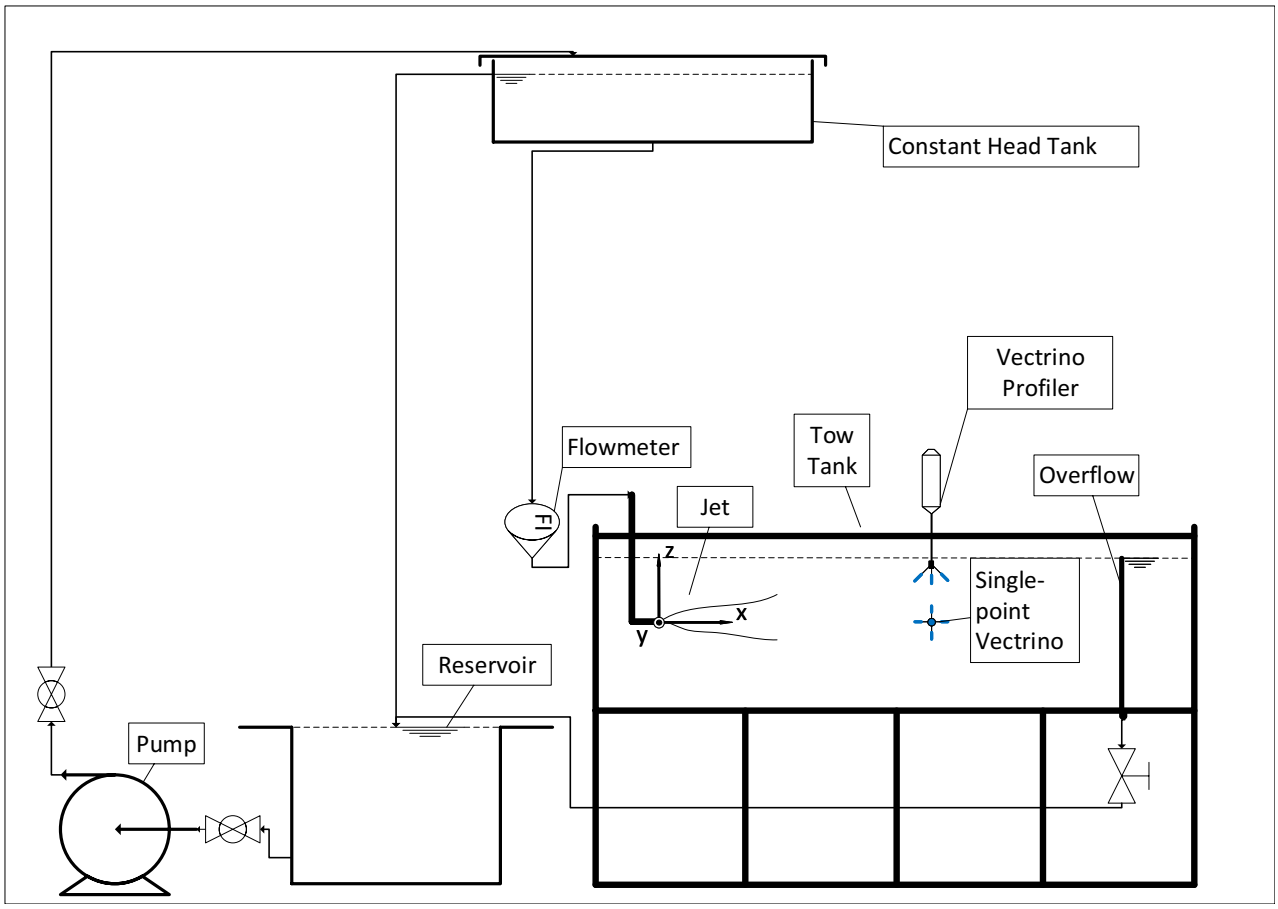

Figure 3–1: Schematic of turbulent jet apparatus for the validation of ADV turbulence measurements (not to scale).

axis, manual traversing mechanism, allowing for translation in the y and z directions, as shown in Figure 3–2. These mechanisms allowed for the relatively accurate alignment of the two ADV sampling volumes. Both of the aforementioned mounting apparatuses were permanently secured to a horizontal beam that could be translated along the length of the tank and bolted into place, thereby facilitating measurements at various downstream locations. Due to the addition of reinforcement features on the tow tank structure, only four mount points could be utilized, corresponding to normalized distances (x/D, where D is the diameter of the jet exit) of 21.6, 31.9, 42.3, and 52.3 from the jet exit to the ADV sampling volumes. It should also be noted that the axial velocity (along the x-axis in Figure 3–1) was measured with the x-beam of both ADVs, while the ADV beams measuring radial velocity (along the y and z-axes in Figure 3–1) were reversed between the two ADVs, given their respective orientations. As the water

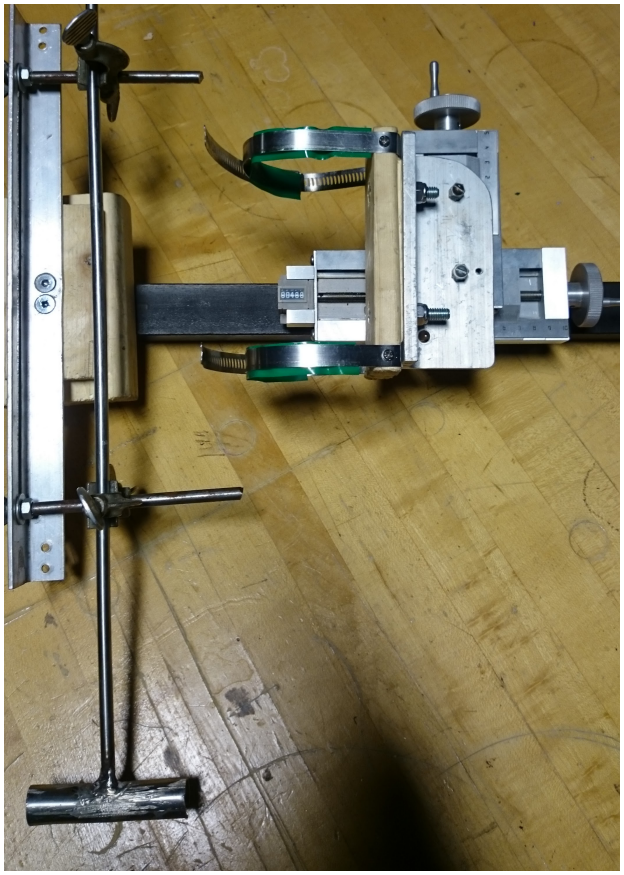

Figure 3–2: ADV mounting apparatus for the jet validation experiments. The construction is similar to that in Figure 2–5, with the Vectrino probe oriented horizontally in a slotted cylinder and the Vectrino Profiler fixed to a support with hose clamps.

used in these experiments was subject to the same filtration mechanism described previously and thus lacking sufficient particles/impurities to ensure adequate signal quality, the system was seeded with Potters Industries Sphericel hollow glass spheres, of 9-13 μm in diameter. To avoid interference between the acoustic signals of the two ADVs, the centreline jet velocity was sampled successively with the Vectrino and Vectrino Profiler for approximately 15 minutes, each, at every downstream location. The ADVs performance and results measured using each instrument were then compared with each other, as well as with theoretical predictions and accepted experimental results, as described in the following section.

3.2 Turbulent jet results

The general performance of the Vectrino Profiler and the ability of the Single-point Vectrino to estimate the dissipation rate have been validated through the analysis of mean

and RMS velocities, probability density functions (PDFs), velocity spectra, and estimates of the dissipation rate, all measured along the centreline of a turbulent jet. In addition, the results illustrate the noise issues inherent to ADV measurements.

The consistency between the two ADVs in the measurement of mean velocities is demonstrated in Figure 3–3, which depicts the downstream evolution of normalized centreline mean axial velocity (where the downstream position is normalized by the jet outlet diameter, and the mean axial velocity is normalized by that of the jet exit, U_0). The agreement between the two ADVs is very good, and there is no indication of either instrument consistently being biased to higher or lower velocity measurements than the other, suggesting the Vectrino Profiler can reproduce the performance of the Single-point Vectrino, at least in the sweet spot of

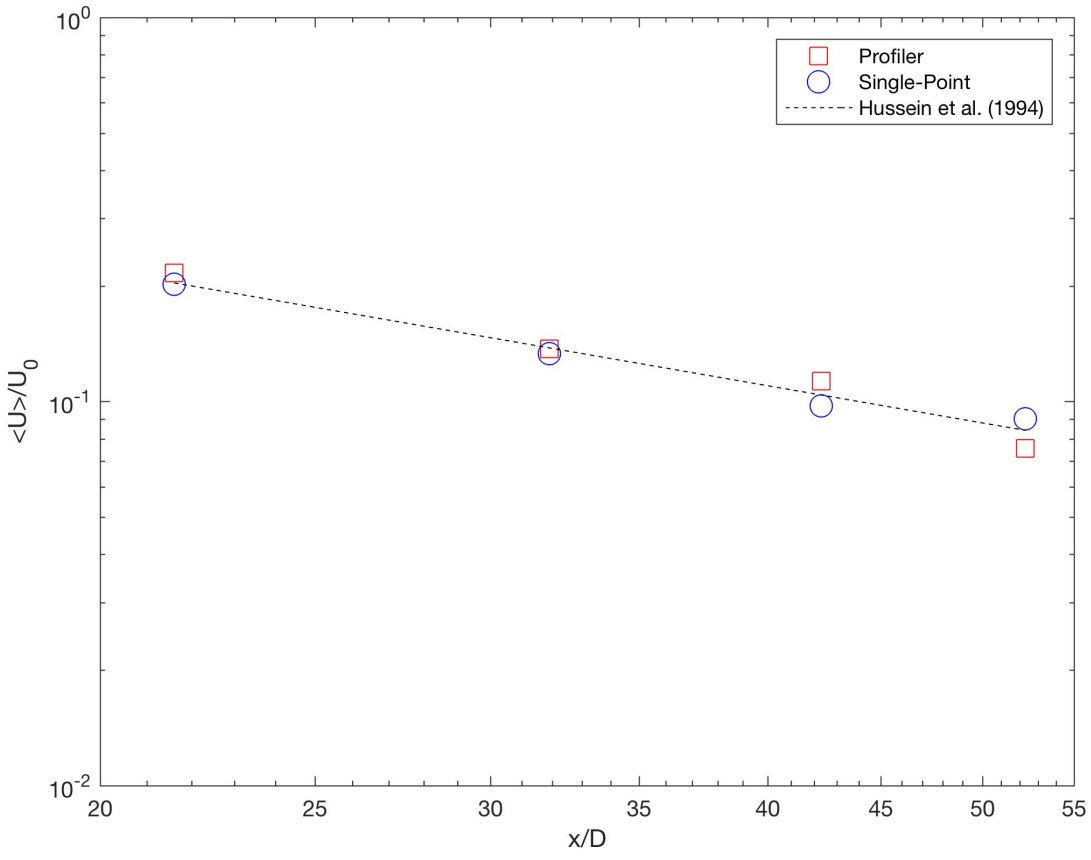

Figure 3–3: Downstream evolution of centreline mean axial velocity. The dotted line is a decaying curve of the form $C_1(\mathrm{x/D})^{-1}$, with $C_1 = 4.4$.

the velocity profile. Furthermore, the measurements of both instruments exhibit an $(x/D)^{-1}$ trend, consistent with theory and past experiments [Hussein et al., 1994], thus demonstrating the ability of the ADVs to accurately measure turbulent flows. However, the non-dimensional coefficient, often referred to as the velocity decay constant, $C_1 = 4.4$, corresponding to the trend of the ADV results is somewhat lower than the value of 5.8 determined by Hussein et al. (1994). The cause of this discrepancy is unclear, however, its value is known to be somewhat sensitive to the virtual origin of the jet, as shown by Khorsandi et al. (2012), which was assumed to be zero in this work. Though this result may suggest an inherent, though unknown, additional issue with Vectrinos or ADVs in general, other factors may account for this difference, such as slight misalignments between the ADV sampling volumes and the jet centreline which have contributed to error throughout these results. Furthermore, the relatively large sampling volumes of ADVs correspond to much lower spatial resolutions than hot-wire and hot-film anemometry techniques, which were used most often in previous studies, including that of Hussein et al. (1994). By sampling over a larger volume, the ADVs may be including off-axis velocities with those at the true centreline, thereby underestimating the mean axial velocity (which is the largest in the jet). It should also be noted that the value of U_0 was calculated based on flowmeter readings of the jet supply (with an uncertainty of $\pm 1.25\%$). Therefore, uncertainty in this value is propagated throughout results where it serves as a normalization parameter. Nevertheless, these results demonstrate the consistency between the performance of the two ADVs, particularly pertaining to the measurement of mean velocities in turbulent flows.

Of equal or greater importance to the study of turbulence, are the abilities of the two ADVs to measure RMS velocities. Comparisons between the three orthogonal RMS velocity components measured by each ADV are presented in Figure 3–4. Because the turbulent round jet is axisymmetric, the radial component of RMS velocity should be constant around the circumference of the jet, thereby justifying the direct comparison of y and z-beam measurements of each ADV (corresponding to v_{rms} and w_{rms}). The results generally show good

agreement between the two instruments over all velocity components and the w_{rms} measurements are consistent with established results obtained using other experimental methods [Hussein et al., 1994, Wygnanksi and Fielder, 1969]. The discrepancy between v_{rms} and w_{rms} values, which, again, should theoretically collapse to the same values, as they both correspond to the radial component of an axisymmetric flow is in agreement with the ADV results of Khorsandi et al. (2012). This is indicative of a source of error inherent to the Vectrinos and similarly constructed ADVs. Specifically, as described in Section 1.3, RMS velocities measured by the x and y-beams of both Vectrinos, tend to be artificially greater than expected, due to the geometry of the corresponding transducers. This phenomenon seems to

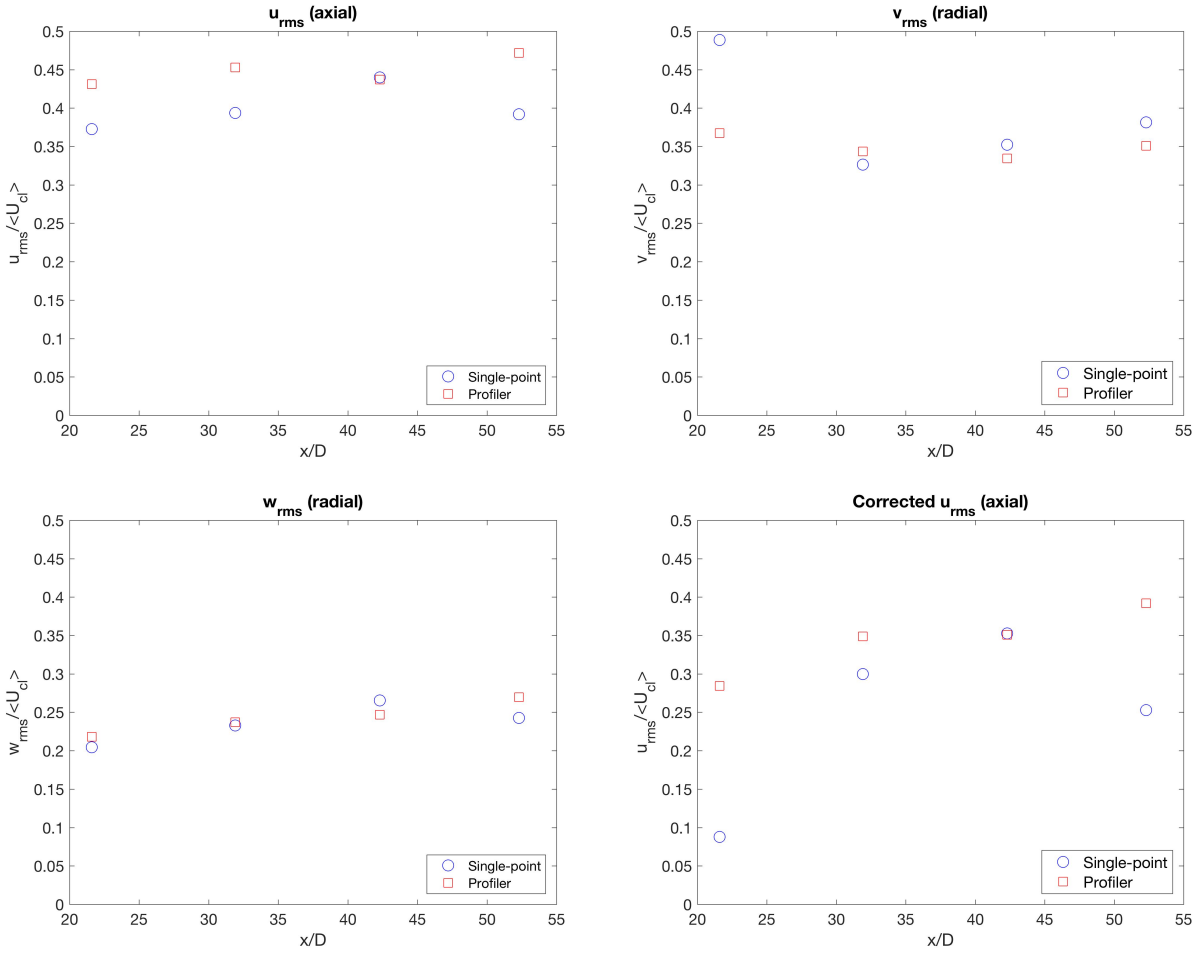

Figure 3–4: Downstream evolution of RMS velocity (comparison between ADVs). The correction to u_{rms} was made using the method of Khorsandi et al. (2012), assuming axisymmetrical flow.

be somewhat exacerbated by the Vectrino Profiler in the case of the axial component, u_{rms}, perhaps due to the added complexity of this instrument, as also evidenced by the findings of Thomas et al. (2017). Finally, the Corrected u_{rms} plot in Figure 3–4 also shows the effect of the noise correction method of Khorsandi et al. (2012) on the axial RMS velocity. This method estimates the noise component of u_{rms} using the difference between the two radial component RMS velocities (again, one of which is measured by the y-beam and the other by the z-beam of each ADV), in a frame of reference aligned with the transducer arms. This change of reference is performed by using the transformation matrix, with which the ADV software converts velocities from transducer-aligned reference frame to Cartesian coordinates, and allows for the accurate separation of noise contributions corresponding to each transducer. Although the overall effect is to reduce u_{rms} closer to accepted values, it has overcompensated or magnified already outlying data points, suggesting that this method should be used cautiously, in settings where no directional bias in signal noise is present (e.g. away from solid surfaces and in flows with well-defined symmetries). Overall, these results further demonstrate consistency between the two ADVs and the accuracy with which the z-beam of each ADV can measure RMS velocities. In addition, the ability of the aforementioned correction method to compensate for geometrical effects of the ADV is substantiated, should the simultaneous measurement of multiple velocity components be required.

Plots of the convergence of the mean and RMS axial velocities, corresponding to measurements from both ADVs at the second downstream location (x/D = 31.9), are provided in Figure 3–5. Velocities were found to have converged to within 1 mm s^{-1}, which is of the same order as the maximum velocity resolution of the ADVs and the RMS background noise in the Vectrino ADV measurements. Given these results, the duration of data sampling at each downstream location was deemed sufficient for the convergence of all relevant turbulence parameters, at this and the other downstream locations.

In addition to convergence analysis, Single-point Vectrino mean and RMS velocity statistics were used to help demonstrate that the fish-filtering method, described in the previous

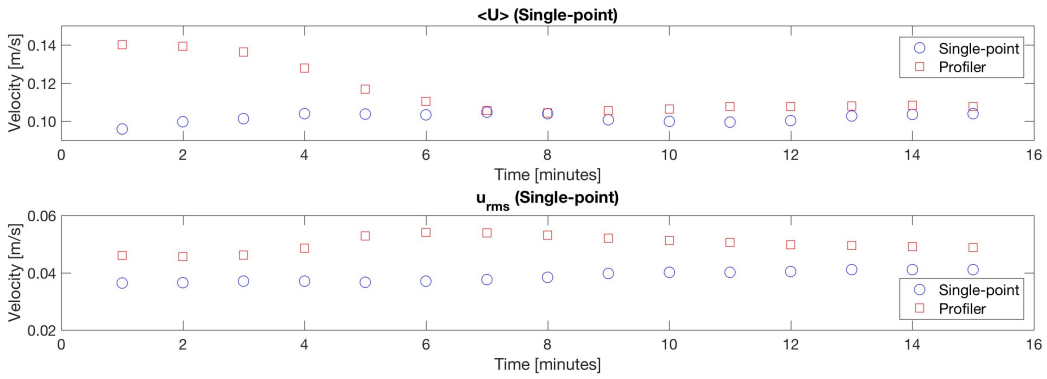

Figure 3–5: Convergence plots of mean and RMS axial velocity at x/D = 31.9 (comparison between ADVs).

chapter, did not inadvertently bias the results of the biogenic turbulence experiments. Velocity time series were filtered first with the corresponding signal criteria noted previously and again with stricter criteria. The first filter application simply ensured that the water was sufficiently seeded (and that the data was of adequate quality overall). The second application (with minimum SNR of 16 dB, correlation of 95%, and amplitude of 100 counts) was used to artificially produce a gappy time series, to allow for the investigation of any effects on turbulence statistics due to the filtering procedure. These overly-stringent filtering criteria produced gappy time series which were qualitatively similar to those resulting from the fish experiments, without compromising the convergence of the data. The mean and RMS velocity statistics corresponding to unfiltered and artificially gappy data sets were consistent, to within 5% in the worst case. Given this consistency, there is no indication that the biogenic turbulence data and its subsequent analysis should be significantly affected by the gappy nature of the data, due to this filtering method.

PDFs of the fluctuating axial centreline component of velocity, measured by both ADVs, are shown in Figure 3–6 at each of the four downstream locations. Both instruments are able to accurately produce the expected bell-shaped, or nearly Gaussian PDFs expected of free-shear flows such as jets [Pope, 2000]. Additionally, the higher levels of noise present in the Vectrino Profiler measurements are further indicated by the greater spread of the PDFs

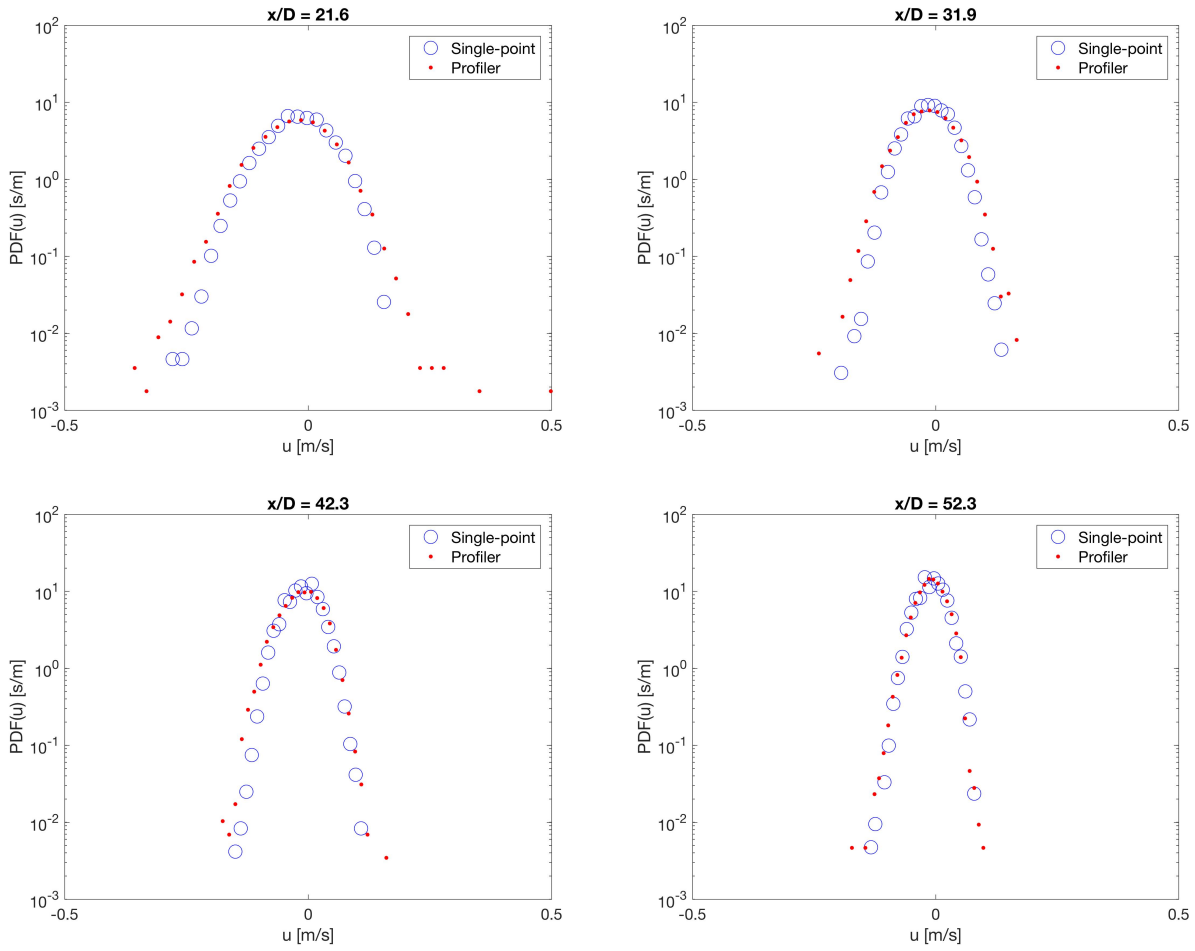

Figure 3–6: PDFs of the fluctuating axial centreline velocity (comparison between ADVs) at 4 downstream locations (x/D = 21.6, 31.9, 42.3, 52.3).

at each downstream location, in contrast to those corresponding to the Single-point ADV. Despite this small disagreement between the instruments, these results further validate the capabilities of the two ADVs to accurately measure turbulent flows.

Power spectra of the fluctuating centreline axial and radial velocities (where the radial component corresponds to the lower-noise, z-beam of the ADV), as measured by each ADV, are depicted in Figures 3–7 and 3–8, respectively. The spectra were calculated using the Bartlett method, with a block length of 1024 data points and a 10% cosine taper window [Press et al., 1996]. A comparison of these spectra provides a clearer view of elevated noise in the Vectrino Profiler measurements, in addition to the noise discrepancies between ADV

velocity components. Particularly, at the first three downstream locations, the Vectrino Profiler spectra are substantially offset from those of the Single-point Vectrino at all frequencies. The shallower decay and higher power of the axial velocity spectra of Figure 3–7 compared to those of Figure 3–8 are also consistent with the findings of Khorsandi et al. (2012), who found that the higher noise in u and v-components of the Single-point Vectrino affect the spectra at all frequencies. Due to this added noise, axial velocity spectra (again, measured using the u-component of the ADV) are generally shallower than the expected -5/3 slope in the inertial subrange, first predicted by Kolmogorov and extensively validated thereafter [Pope, 2000]. The radial velocity spectra however, again, measured with the low-noise w-component, agree

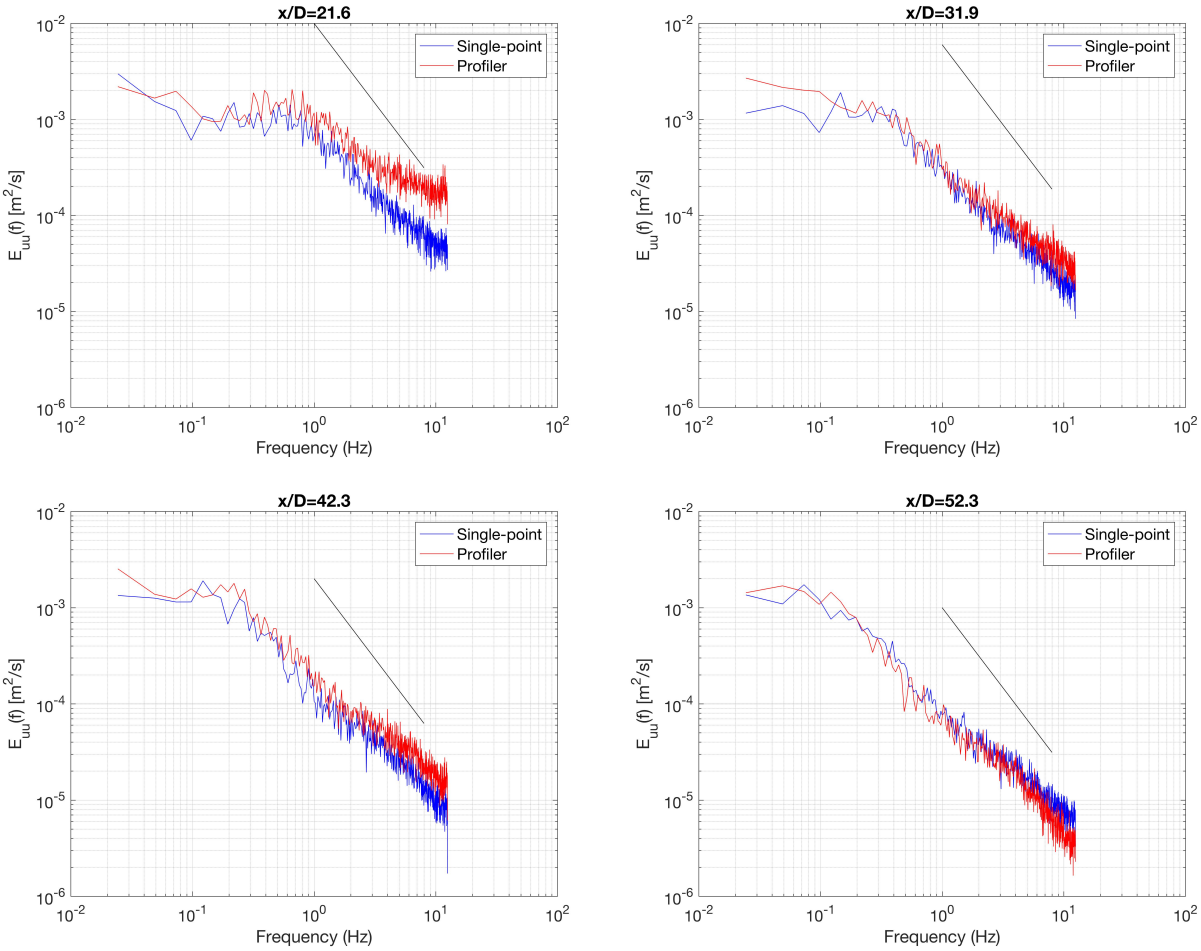

Figure 3–7: Turbulent axial centreline velocity spectra at the four downstream locations (comparison between ADVs), where the diagonal line has a slope of -5/3.

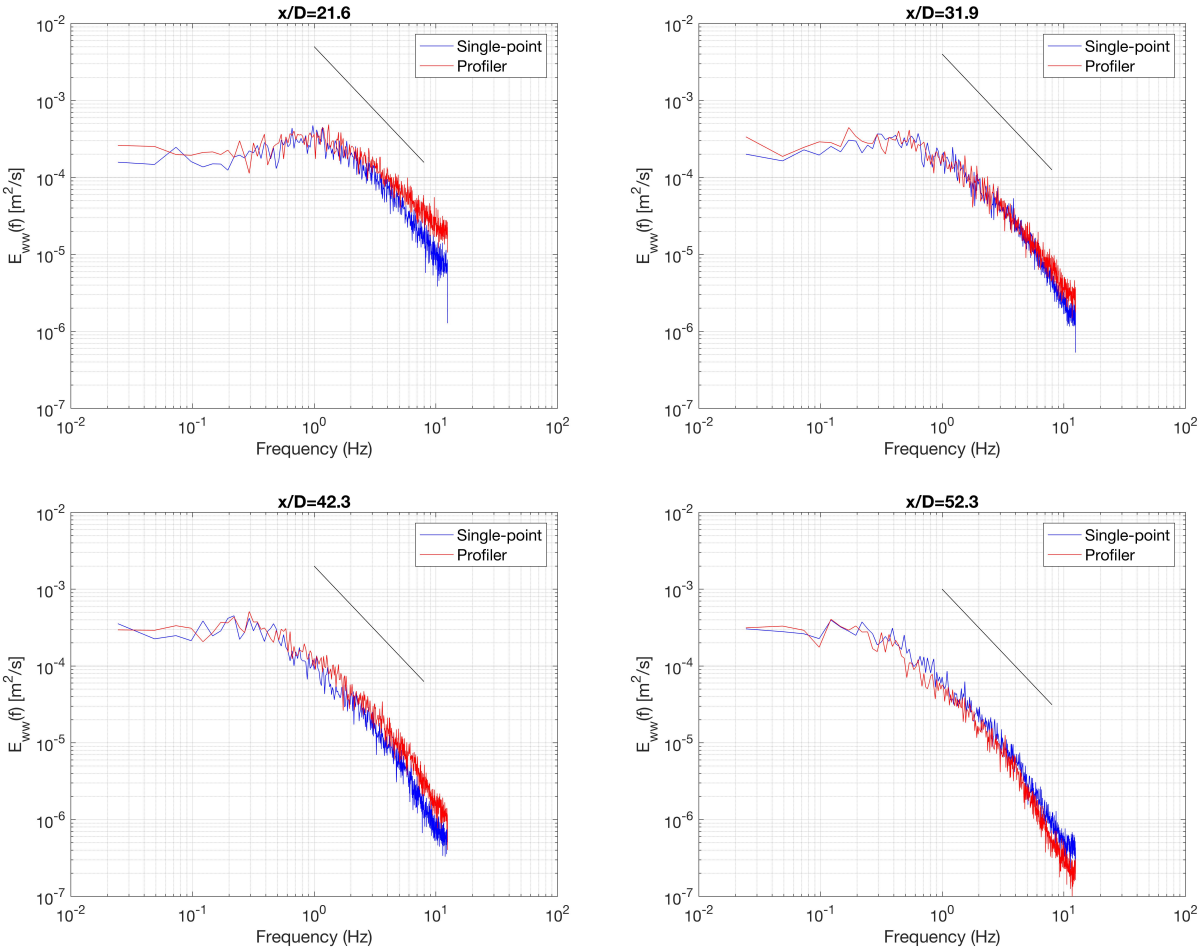

Figure 3–8: Turbulent radial centreline velocity spectra at the four downstream locations (comparison between ADVs), where the diagonal line has a slope of -5/3.

much better with the expected slope, though with the same offset between ADVs noted for the axial velocity spectra. Regardless, velocities measured with the w-component of both ADVs can provide turbulence spectra with reasonable confidence, which will serve to better characterize flows such as biogenic turbulence.

Given the above results, it is clear that the ADVs in question are relatively consistent in the measurement of mean and RMS velocities, and can replicate accepted downstream trends of these parameters. In particular, and consistent with research, the present validation demonstrates that the w-component of the ADV measurements are the most reliable and should be used exclusive of the other velocity components in the subsequent analysis of

biogenic turbulence, whenever possible. By confirming the validity of the assumption that biogenic turbulence is approximately isotropic, as discussed in the next chapter, only one velocity component is needed for much of this analysis.

Although the accurate measurement of velocity is important in the study of biogenic turbulence, the ability to reliably estimate the dissipation rate is crucial, for the accurate quantitative assessment of the contribution of swimming animals to the ocean energy budget. As well, the validation of the ability of simpler, less-expensive, point measurement ADVs, such as the Single-point Vectrino, to estimate the dissipation rate, using large-scale quantities, may allow for the further analysis of both historical data collected using such instruments and future biogenic turbulence studies where profiling ADVs or other devices are either not available or impractical. For example, in circumstances such as those of this study, the Single-point Vectrino was the predominant instrument used for the Congo tetra experiments, due to practical constraints, and because the Vectrino Profiler would have produced too much noise to accurately capture the velocity fluctuations induced by the smallest animals, in this case the neon tetras. With this in mind, estimates of the dissipation rate along the centreline of the jet, as measured more directly by the Vectrino Profiler, and estimated from large-scale parameters by the Single-point Vectrino are compared in Figure 3–9 and benchmarked against an accepted downstream trend [Antonia et al., 1980]. The dissipation rate was estimated using the Vectrino Profiler data assuming locally homogeneous flow (which is less restrictive than the more commonly used homogeneous and isotropic assumption) and therefore Equation 1.7 (in the coordinates of the Vectrino Profiler: $\epsilon = 3\nu\left(\overline{\left(\frac{\partial u}{\partial z}\right)^2} + \overline{\left(\frac{\partial v}{\partial z}\right)^2} + \overline{\left(\frac{\partial w}{\partial z}\right)^2}\right)$) was implemented with second order finite differences as approximations to the velocity gradients. These results are in excellent agreement with the results of Antonia et al. (1980) as well as previous studies cited therein and, importantly, help to confirm the ability of the Vectrino Profiler to properly measure dissipation rate in a fundamental turbulent flow. Perhaps more importantly to the subsequent biogenic turbulence analysis, the Single-point Vectrino was also able to demonstrate the downstream decay of dissipation using Equation 1.9 (specific

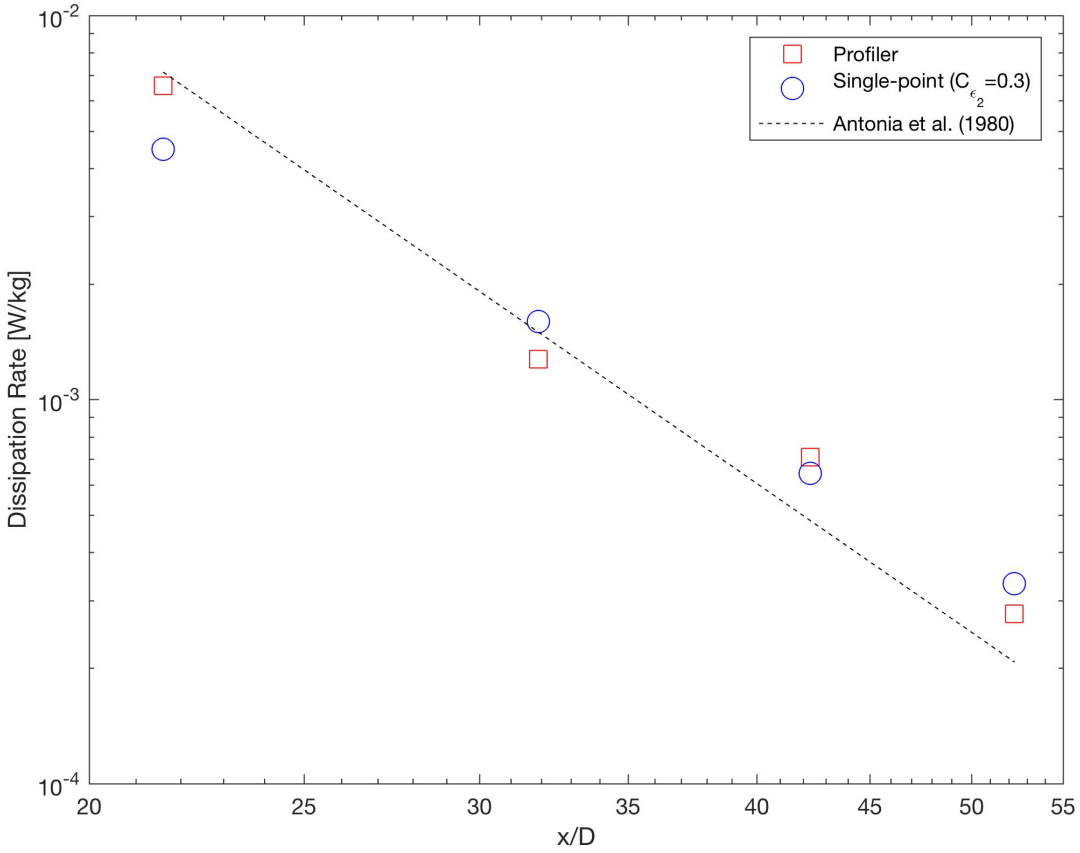

Figure 3–9: Downstream evolution of centreline dissipation rate (comparison between ADVs). The dotted line is the accepted $48\frac{U_0^3}{d}(x/D)^{-4}$ relation [Antonia et al., 1980].

to this experiment: $\epsilon \sim C_{\epsilon_2}\frac{u_{rms}^2}{T}$, where $C_{\epsilon_2} = 0.3$). The integral time scale in this case is estimated by integrating the autocorrelation coefficient curves of the fluctuating centreline axial velocity, which are shown in Figure 3–10, and, for consistency, the centreline axial RMS velocity was used as the representative component in the numerator of Equation 1.9. Although the curves generally decay with the expected shape for homogeneous turbulence, they tend to plateau above zero, instead of the more typical overshoot of the x-axis and subsequent settling around zero [Tennekes and Lumley, 1972]. Therefore, to avoid incorrectly large integral time scale estimates, the curves were integrated (using the trapezoid method [Burden and Faires, 2011]) only to the first local minimum of $\rho(\tau)$ (i.e. the point at which the slope became zero). Returning to the dissipation results, although the Single-point Vectrino

demonstrates the appropriate trend, the results exhibit a slightly smaller scaling coefficient ($C_{\epsilon_2} = 0.3$) than the C_{ϵ_1} values of previous work, which are generally in the range of 0.5-1.1 [Vassilicos, 2015]. Although there is no theoretical stipulation that these coefficients should be identical, they should at least be of the same order of magnitude, so as to be consistent with the arguments of Taylor (1935). The disparity between C_ϵ values may be due to the overestimation of u_{rms} by the ADV, however, it is unclear how the additional noise contributing to this overestimation also affects the integral time scale estimate used in these results. Additionally, the time scale used in Equation 1.9 is generally taken to be the Lagrangian time scale, as opposed to the Eulerian time scale measured by the stationary ADV [Taylor, 1935].

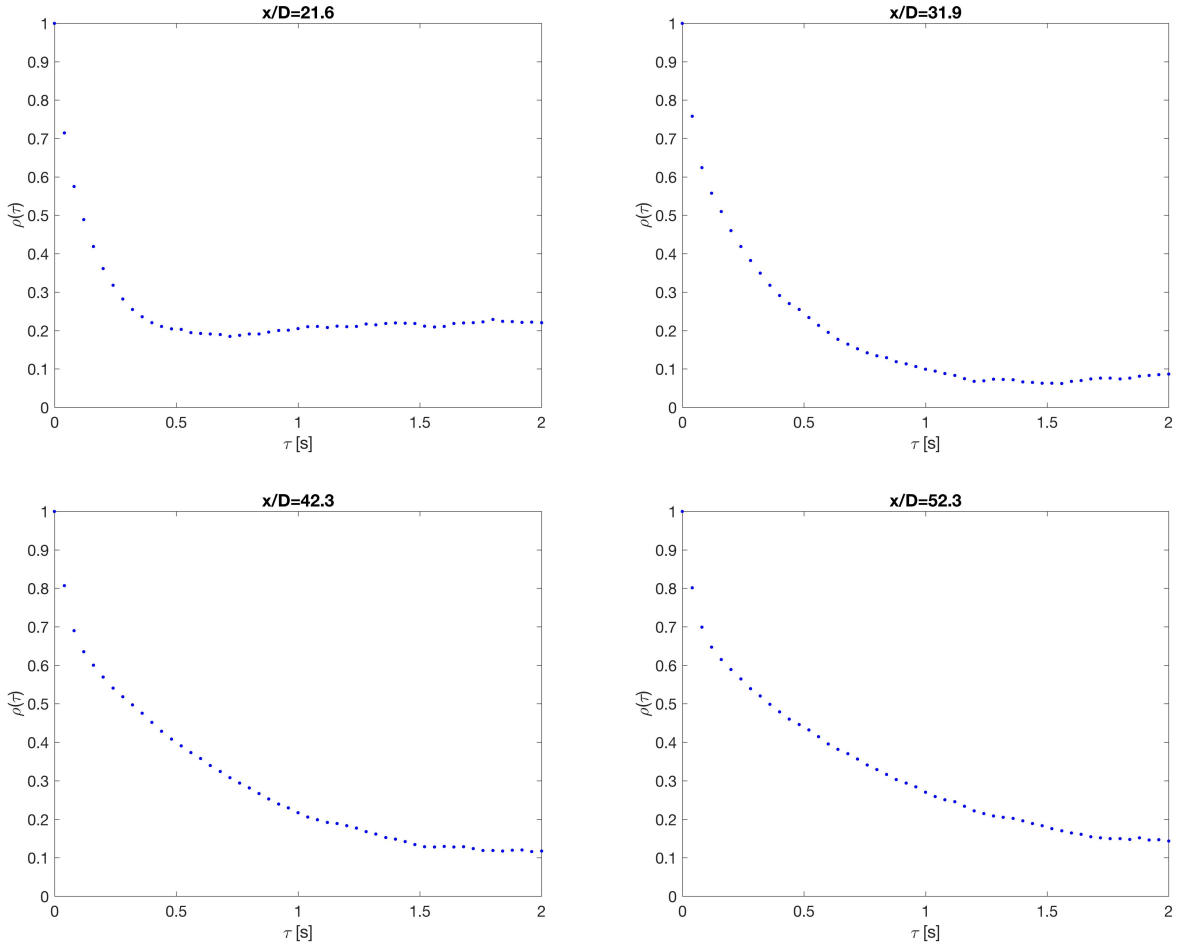

Figure 3–10: Sample autocorrelation coefficient plots of the fluctuating axial velocity, measured by the Single-point Vectrino, at each downstream location.

Corrsin (1963) provides physical and theoretical arguments to suggest that these two scales are not necessarily equal, but directly proportional to each other within a constant, which may be dependant on turbulence intensity and is to be measured experimentally. As a detailed study of this constant is beyond the scope of this work, it is assumed to be unity, as approximated by previous work, though with the knowledge that the Eulerian integral time scale may be a slight underestimate for dissipation rate calculations [Corrsin, 1963]. Nevertheless, it is clear that the Single-point Vectrino can readily estimate the order of magnitude of the dissipation rate of biogenic turbulence.

Given the relative consistency between the results of the two ADVs discussed, the Vectrino Profiler has been shown to be a relatively accurate tool for turbulence measurements, despite increased noise levels as compared to those of the simpler Single-point Vectrino. The Vectrino Profiler may be an important tool in future biogenic turbulence applications where the measurement of spatial velocity gradients are essential. However, the Single-point Vectrinos demonstrated ability to accurately reproduce the expected forms of downstream velocity evolutions, PDFs, velocity spectra and, most importantly, dissipation rates, all with lower noise contributions than the Vectrino Profiler, also render it an appropriate instrument for the study of biogenic turbulence, particularly in aggregations where the turbulent Reynolds number and velocity fluctuations are relatively small.

CHAPTER 4
Results and discussion

The results of the experiments with the two species of tetra are analysed herein and presented in the context of three related topics. First, the general nature of biogenic turbulence within a school of Congo tetras is explored, to both test the assumption that it is approximately isotropic, and to demonstrate its similarity to that of more extensively investigated turbulent flows. Second, the impact of biological factors, such as abundance and animal size, are assessed, with attention given to practical considerations for the use of ADVs to measure biogenic turbulence. Finally, the results are compared to the typical levels of background turbulence found in lakes and oceans, to estimate the potential significance of biogenic turbulence in aquatic environments. It should be noted that all of the current measurements presented in this chapter were obtained using the Single-point Vectrino, unless explicitly stated, with the procedures outlined in Chapter 2.

4.1 Structure of biogenic turbulence

The assumption of isotropy of biogenic turbulence has been used extensively throughout past literature [Katija, 2012]. In this context, however, such stipulations of global isotropy have most often been out of necessity, to allow for the estimation of the dissipation rate using instruments capable of measuring a velocity gradient in only one dimension (i.e. necessitating the use of Equation 1.8). Despite the prevalence of this assumption, its validity has not been investigated experimentally, particularly for the simple case of a stationary aggregation of animals. Furthermore, it is unclear whether the biogenic turbulence observed in such aggregations is even fundamentally similar to that of more classic examples of isotropic turbulence, and under what circumstances this may be the case. Given these uncertainties, experiments conducted within the school of Congo tetras using the Single-point Vectrino have allowed for the comparison of horizontal and vertical velocity components, calculation

of PDFs of the fluctuating component of velocity, and the velocity spectra in order to shed light on the structure of biogenic turbulence under these basic conditions.

By using the two mounting configurations of the Single-point Vectrino described in Chapter 2, the horizontal and vertical components of velocity were measured using the low-noise, z-beam of the ADV. The first result of these experiments is summarized in Table 4–1, which compares the RMS velocities in the vertical and horizontal directions. Although the ratio of RMS velocities is not exactly unity, the measured value of 0.84 is close enough to confidently assume approximate isotropy, at least for order of magnitude estimates of biogenic turbulence parameters. The strict minimum abundance of 1250 animals/m^3, imposed while the ADV was in its vertical orientation using the Plexiglas tank dividers, could not be implemented in the same manner, with the ADV in the horizontal configuration. However, the school exhibited the same size and structure throughout all experiments and remained in the same location relative to the ADV probe, regardless of its orientation. It should be noted that this level of abundance is approximately that quoted by Huntley and Zhou (2004) for the similarly sized Japanese anchovy, and is close to the natural abundance generally observed in the Congo tetra tank. In practical terms, the demonstration of the approximate isotropy of biogenic turbulence has aided in validating past measurements and will simplify subsequent analyses. For example, this result will allow the measurement of *TKE* and estimation of dissipation rate, using velocity data solely obtained with the low-noise z-beam data of the the Single-point Vectrino.

In addition to RMS velocities, the power spectra of the fluctuating w-component of velocity (measured by the z-beam) are shown in Figure 4–1, both of which are compared with

Velocity [m s^{-1}]	Vertical Component	Horizontal Component	Ratio
RMS	0.0061	0.0073	0.84

Table 4–1: Comparison of velocity components, both measured by the z-beam of the Single-point Vectrino, using the vertical and horizontal configurations, respectively, as depicted in Figure 2–5. Measurements were made in the Congo tetra school at a minimum abundance of 1250 animals/m^3.

the -5/3 decay line expected in the inertial subrange of high Reynolds number turbulence [Pope, 2000]. The measured spectra demonstrate excellent agreement with the expected decay, although the spectra of the vertical component contains a spike at intermediate frequencies, suggesting the presence of an oscillatory component of the flow. This may correspond to the strong vortices produced by the motion of the tail fin of fish as they exit or swim near the sampling volume, the possibility of which is further discussed in the following section. The spectra presented do not exhibit the same roll-off observed by Tanaka et al. (2017), at low wavenumbers, which is presumably due to the fact the lowest frequencies were not accessible in the current analysis, given that long interrupted time series where not capable of being measured. The gappy nature of the data, as discussed in Section 2.3, only allowed for block lengths of 64 and 32 data points, sampled at 25 Hz, in the vertical and horizontal directions, respectively, while still ensuring convergence was achieved at all frequencies in the spectra. The effects of using relatively small continuous segments of data, generally of variable length, are discussed in the following chapter. Regardless of these complications, the consistency between the horizontal and vertical spectra provides further support to the assumption of isotropy and the approximate -5/3 slope of the spectra give credence to the treatment of biogenic turbulence in the same manner as that of more common turbulent flows.

To further corroborate the consistency between biogenic and physical turbulence, a PDF of the fluctuating vertical component of velocity, representative, in its general shape, of the Congo Tetra measurements at all abundances, is shown in Figure 4–2. In this case, data was used from the experiments in which the ADV was in the vertical orientation. The form of the PDF is consistent with the expected, approximately Gaussian, shape characteristic of homogeneous turbulence [Pope, 2000]. The peaks at the edges of the PDF can be attributed to erroneous velocity spikes inherent to ADV measurements, however, because such velocity spikes, which remained after the filtering for interference of the fish swimming through the sampling volume, were so rare, no despiking methods were used in the data analysis

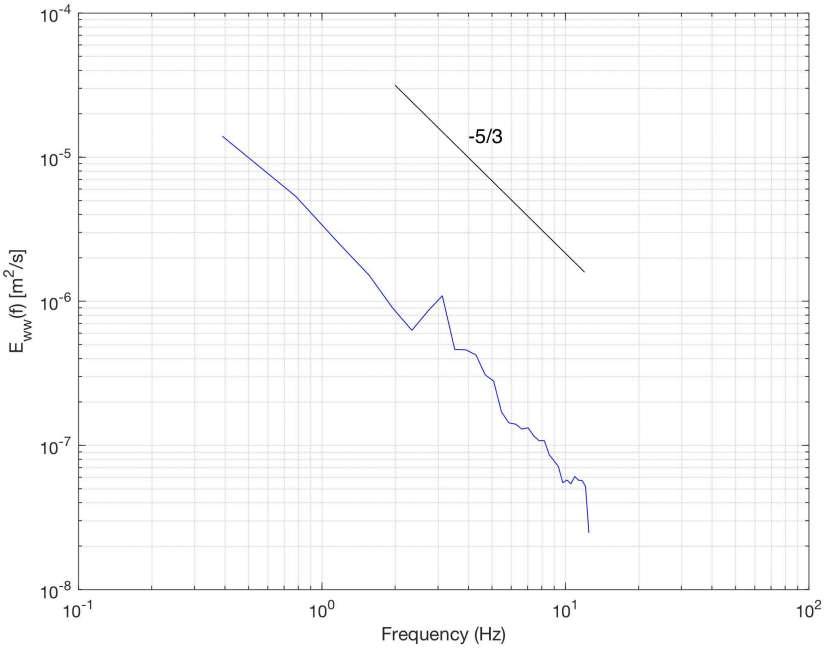

(a) vertical component

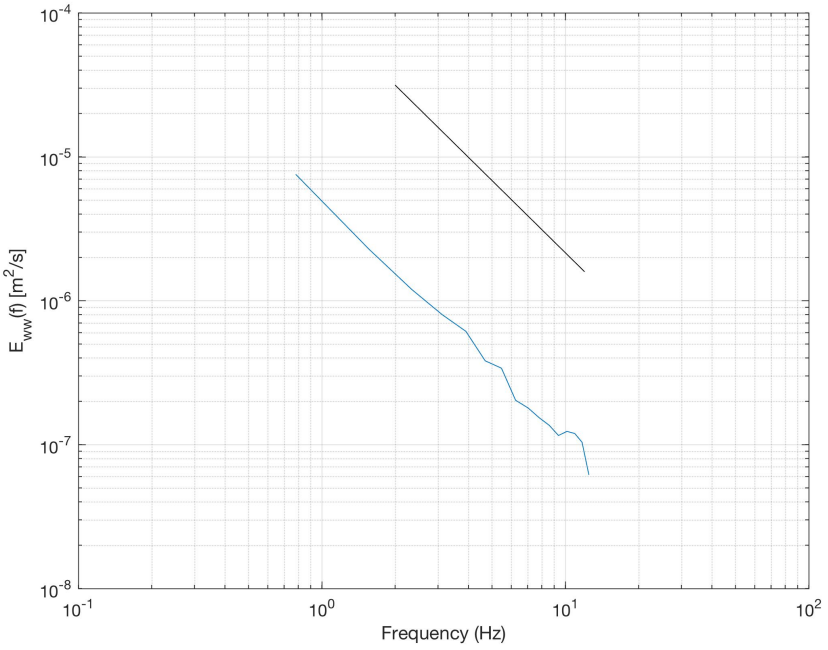

(b) horizontal component

Figure 4–1: Power spectra of the fluctuating velocity, measured by the z-beam of the Single-point Vectrino, within a school of Congo tetras at a minimum abundance of 1250 animals/m^3.

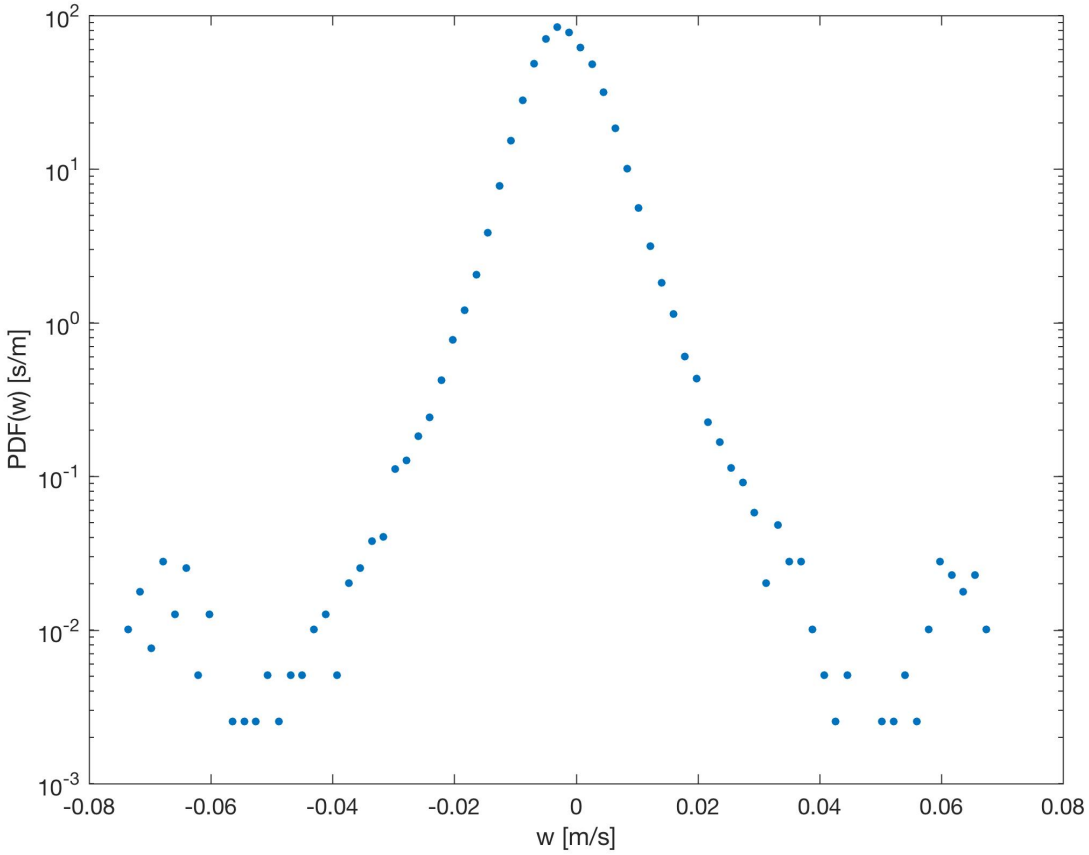

Figure 4–2: PDF of the fluctuating w-component of velocity, within a school of Congo tetras at a minimum abundance of 1250 animals/m^3.

procedure [Goring and Nikora, 2002]. Nevertheless, this result garners further evidence for the similarity between biogenic turbulence, at typical schooling abundances, and physically induced homogeneous turbulence.

PDFs of the fluctuating vertical component of velocity, measured at the two extremes of the abundance range used in this work, are also shown in Figure 4–3. Similar to that above, these PDFs exhibit an approximately Gaussian form, suggesting that the lowest abundance tested still contains a sufficient density of moving animals to sustain homogeneous turbulence and the highest abundance does not overcrowd the fish to the point of being stationary. This similarity of turbulence parameters across abundance levels is examined in more detail in the following section. It may be noted, that at significantly lower abundances than those

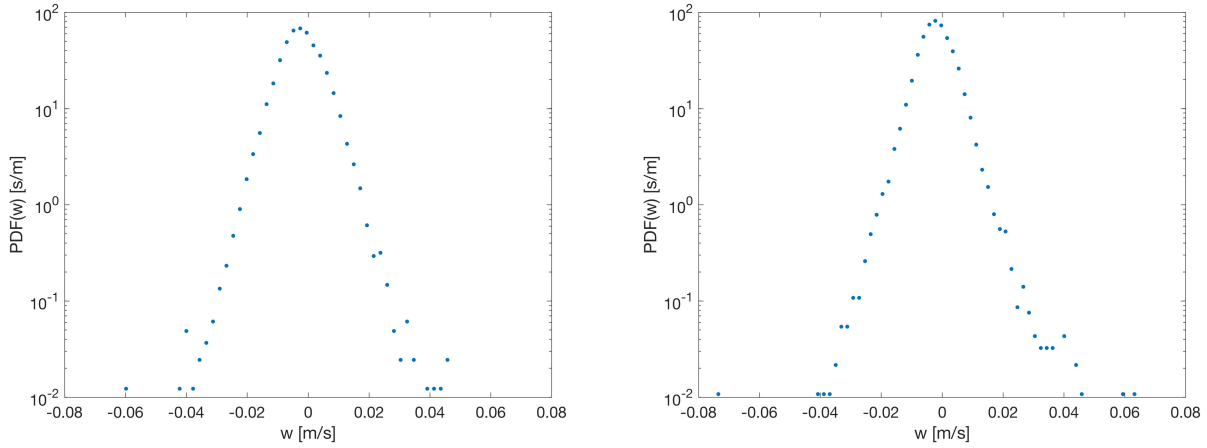

Figure 4–3: PDFs of the fluctuating w-component of velocity, within a school of Congo tetras at two extremes of minimum abundance.

examined in this work, where the average animal spacing is many times the average body length, it is unclear whether or not the animal wakes will interact, or influence enough of the fluid domain, to consistently sustain homogeneous turbulence. However, given the consistent Gaussian forms of the PDFs across the abundance range of this study, the same analytical methods may be applied to the data at each abundance with reasonable confidence.

Despite the limitations imposed by the gappy nature of the velocity time series, on the basis of the similarity between RMS velocity components and fluctuating velocity spectra, the approximately -5/3 decay of these spectra, and the quasi-Gaussian form of the fluctuating velocity PDF, biogenic turbulence can be reasonably approximated as isotropic. The significance of these results, however, must also be examined in the context of the various biological factors that may affect the general structure of biogenic turbulence, as discussed in the following section.

4.2 Biological factors

As described above, biogenic turbulence exhibits important characteristics of the more typically studied physically forced turbulence. However, whether such results are quantitatively consistent over a range of abundances and animal sizes remains unclear. The effect of abundance on various turbulence parameters has not previously been rigorously evaluated,

therefore it is discussed here using the Congo tetra measurements. Moreover, in practical terms, the smallest animal sizes and/or lowest abundance levels producing biogenic turbulence, which can be accurately studied using ADVs, have yet to be determined, and are also investigated below. Lastly, the results of the current work with neon and Congo tetras are examined and compared to past measurements of biogenic turbulence, despite the added levels of complexity and uncertainty present in much of that data.

Results pertaining to the Congo tetra experiments, at each of the six abundances investigated, are summarized in Table 4–2. With the exception of U (which is not affected by the inherent ADV noise issues), all of the results correspond to the w-component data (measured by the low-noise z-beam of the Vectrino), such that, assuming isotropy, $TKE = \frac{3}{2}w_{rms}^2$ and $\epsilon = C_{\epsilon_2}\frac{w_{rms}^2}{T}$, where $C_{\epsilon_2} = 0.3$. It should also be noted that T is estimated using a minimum data segment length of 50 points for autocorrelation calculations, the implications of which are discussed following these results. From the data presented, no obvious relationship can be discerned between the abundance level and any of the turbulence parameters. Although

A [No/m^3]	U [m s^{-1}]	w_{rms} [m s^{-1}]	TKE [m^2 s^{-2}]	T [s]	ϵ [W kg^{-1}]
500	-1.6×10^{-3}	6.7×10^{-3}	6.5×10^{-5}	0.21	6.3×10^{-5}
750	-1.5×10^{-3}	7.4×10^{-3}	8.1×10^{-5}	0.19	9.0×10^{-5}
1000	-1.6×10^{-3}	6.2×10^{-3}	5.6×10^{-5}	0.22	5.4×10^{-5}
1250	-1.6×10^{-4}	6.1×10^{-3}	5.2×10^{-5}	0.25	4.2×10^{-5}
1500	-8.8×10^{-4}	6.5×10^{-3}	6.1×10^{-5}	0.21	6.0×10^{-5}
1750	-2.4×10^{-4}	5.8×10^{-3}	4.8×10^{-5}	0.21	4.8×10^{-5}

Table 4–2: Dependence of turbulence parameters measured within the Congo tetra school on abundance.

no past research has demonstrated that such a relationship should exist, the predictions of Huntley and Zhou (2004) incorporated what were thought to be typical abundances for a variety of species to arrive at dissipation rate estimates. The fact that such predictions may be invariant over a range of abundances suggests the existence of other important factors not accounted for in this past work. The current work suggests that the expected effects of abundance are offset by those of behaviour, at least for abundances which are sufficiently

high to support the generation of turbulence. For example, it is possible that at lower abundance, fish are more likely to swim faster and over longer trajectories, while at the highest abundance, swimming speed and trajectory length are suppressed by crowding, leading to more of a 'stop-start' type of motion. The qualitative observations of the fish behaviour, made during the experiments, support these hypotheses, particularly that of the differences in trajectory length. Specifically, at low abundance, the fish could more often be observed circulating the tank in a structured aggregation (i.e. more closely resembling a 'shoal', where the swimming direction of each fish is aligned with those of its neighbours and spacing between animals is more consistent), in a counter-clockwise direction as viewed from above the waters surface. For example, at the two lowest abundance levels, the aggregation did not necessarily spread throughout the entire tank volume, but occasionally spread throughout a relatively thin depth range below the probe head, or moved as a unit between opposite halves of the tank length. Whereas at higher abundance, particularly the two uppermost values, trajectories tended to be random and change direction abruptly. Although a detailed comparison between these behavioural observations of fish in captivity with abundance dependant behaviours exhibited in the wild was beyond the scope of this work, future work may need to account for any discrepancies should laboratory results be used to predict levels of biogenic turbulence in natural environments. Additionally, a wider variety of school and tank sizes may help to determine more precisely the effects of spacial constraints on behaviour. Finally, the construction of these experiments is designed to provide a snapshot of a larger stationary group of animals rather than a singular point in the ocean. Whereas in the real ocean, it may be more likely that significant biogenic mixing events may correspond to animals undergoing some form of concerted migration, which may affect turbulence production in an unknown manner.

Despite the apparent complexity in these experiments, a representative convergence plot for these data, shown in Figure 4–4, for w_{rms}, demonstrates that the velocity has converged

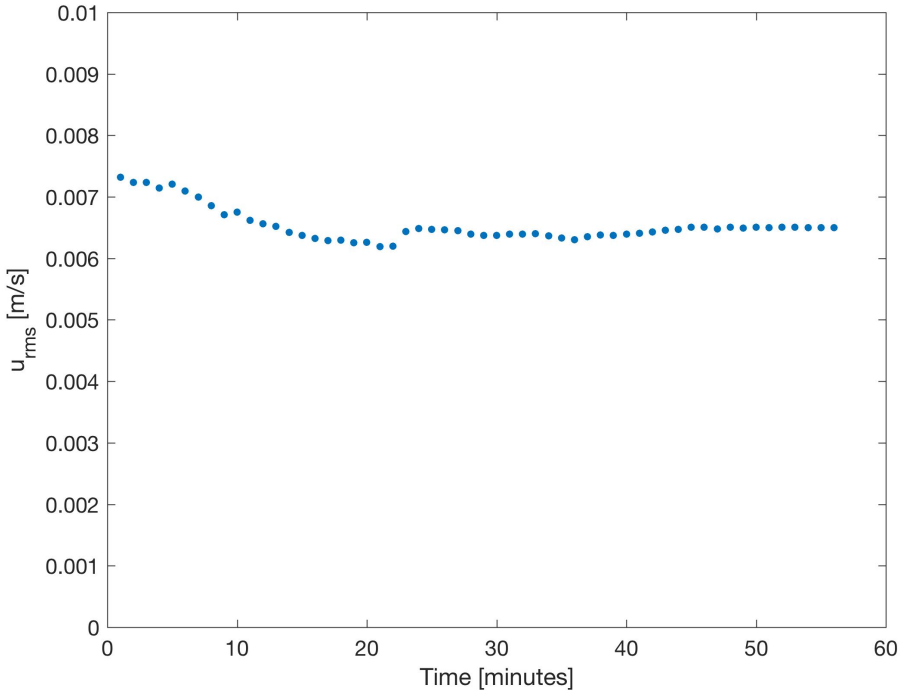

Figure 4–4: Convergence of w_{rms} measured within the Congo tetra school over three experiments at an abundance of 1500 animals/m^3.

to within 10^{-4} m s^{-1}, close to the maximum resolution of the Single-point Vectrino. Additionally, the proposed differences in swimming speed, however, could not be quantified by simply observing by eye, and in general, behavioural effects such as aggregation structure and swimming speed would be best studied through object recognition and tracking technology, which was beyond the scope of this work. A further complication to the dissipation rate results is the way in which the gappy nature of the data affected the estimation of the integral time scale.

As the autocorrelation curves are used to estimate the integral time scale, and, by extension, the dissipation rate, this complication impacts the main results of this work. The effects of the gappy time series were investigated, as shown in Figure 4–5, by increasing the minimum length of the data segments to calculate the autocorrelation. These data demonstrate a strong relationship between the shape and decay of autocorrelation curves and the length of the data segments (sequences of uninterrupted velocity readings) used

to calculate them. Specifically, the first zero of the autocorrelation curve is forced further to the right (i.e. to higher values of time lag). This trend is consistent over the range of abundances investigated, and clearly, the individual curves have not asymptoted, nor show signs of doing so, to a steady shape for the range of minimum segment lengths presented. Additionally, the bumps in the autocorrelation curves corresponding to the larger segment

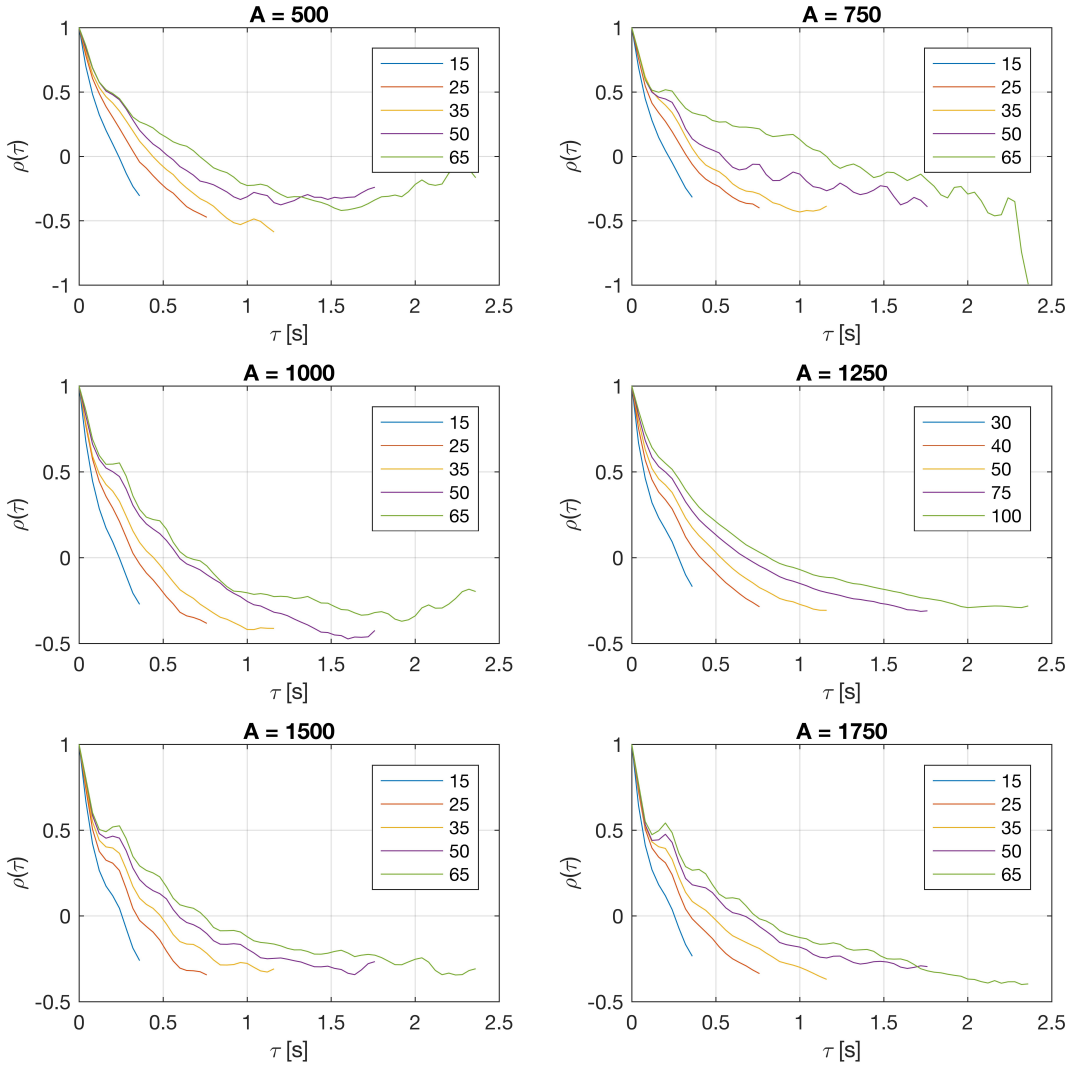

Figure 4–5: Effect of minimum length of data segment on the autocorrelation coefficient of the fluctuating w-component of velocity within Congo tetra schools of abundances ranging from 500 to 1750 animals/m^3.

lengths may be further evidence of the oscillatory motion hypothesized in the previous section, in reference to the spike in the velocity spectra. This investigation is limited by the fact that increasingly longer segments occur increasingly rarely, so that the individual points along autocorrelation curves are no longer converged at the highest minimum segment lengths. A minimum segment length of 100 data points was attainable at the 1250 animals/m^3 level, due to the fact approximately three times the amount of data was recorded at this abundance, compared to the five others, thus capturing more instances of relatively long data segments. However, because the general trend remains consistent with the other abundances and much larger segments were found to be virtually impossible to observe in these schools, performing additional experiments at the other abundance levels was deemed to be not beneficial.

The corresponding trend between the integral time scale and minimum segment length is illustrated in Figure 4–6, where, similarly to the autocorrelation results, the values of the integral time scale are not asymptotic in the range of minimum segment lengths used. The near collapse of all of the trends is consistent with the previous finding that turbulence parameters are seemingly independent of abundance within the range employed herein. A minimum segment length of 50 consecutive data points was used for the results presented, as it was the largest value that produced converged autocorrelation curves at all abundances, and as the idealized calculation of the integral time scale corresponds to the autocorrelation of an infinitely long time series. However, there remains substantial uncertainty in the integral time scale and dissipation rate results, given the fact that if the trend of increasing integral time scales demonstrated in Figure 4–6 were to continue to much larger data segment lengths, the dissipation rates presented would tend to be overestimated. However, as shown in Table 4–3, the dissipation rate estimates made using 50 point minimum data segments tend to be underestimates, of up to nearly a factor of 4, compared to those determined from preliminary measurements of velocity gradients using the Vectrino Profiler. Therefore, the Single-point Vectrino may be considered an adequate tool for the purposes of order of magnitude estimates of dissipation rates, given appropriate attention to the effects of gappy time series data; a

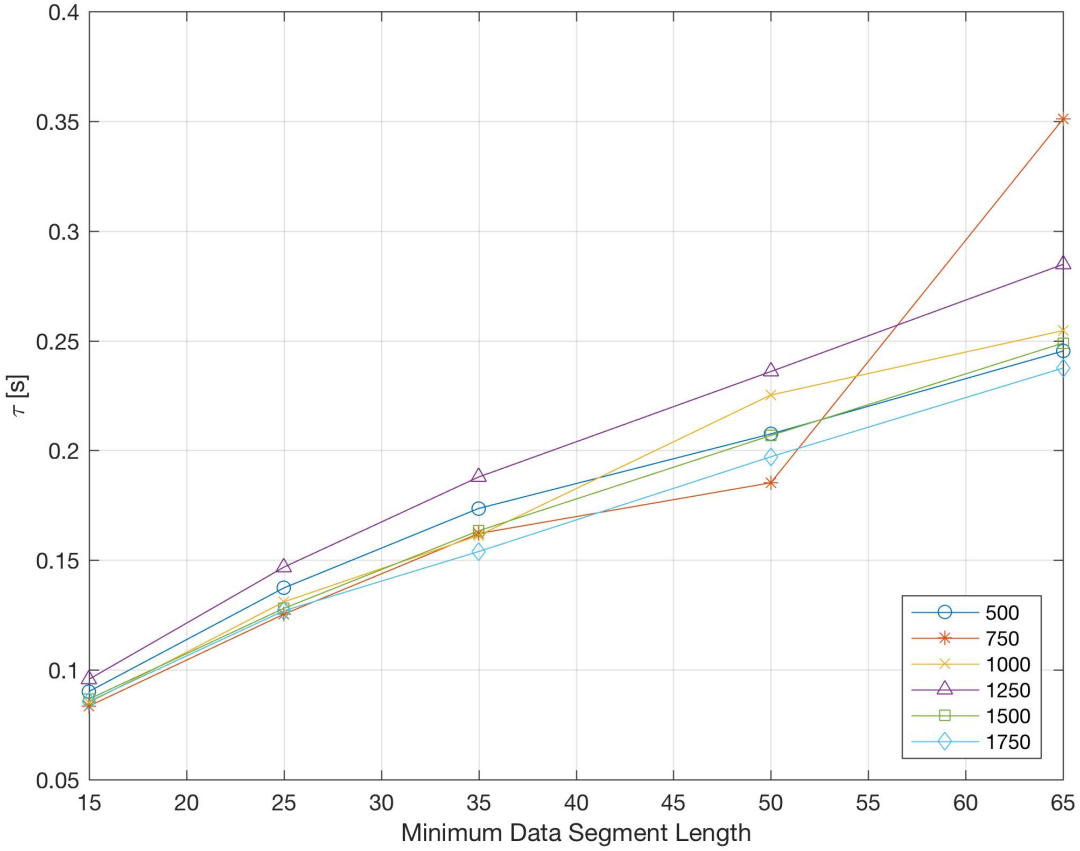

Figure 4–6: Effect of the minimum data segment length on the integral time scale within Congo tetra schools of abundances ranging from 500 to 1750 animals/m^3.

topic which may require further theoretical and experimental investigation if more accurate integral time scale estimates are desired. Given these results, the effects of body size may be examined as another factor that will influence the generation of biogenic turbulence and the feasibility of its measurement, adding another layer of complexity to its understanding.

ϵ [W kg^{-1}]	Single-point Vectrino	Vectrino Profiler
$15\nu\overline{\left(\frac{\partial w}{\partial z}\right)^2}$	-	1.6×10^{-4}
$C_{\epsilon_2}\frac{w_{rms}^2}{T}$	4.2×10^{-5}	6.6×10^{-5}

Table 4–3: Comparison of estimates of dissipation rate, made by each ADV, with the Congo tetra school at an abundance of 1250 animals/m^3. The minimum segment lengths used for the estimates of the integral time scale were 50 points for the Single-point Vectrino and 200 points for the Vectrino Profiler (i.e. segments corresponding to 2 s, given the respective sampling frequencies of 25 Hz and 100 Hz) and $C_{\epsilon_2} = 0.3$.

To assess the role of body size in the generation of biogenic turbulence, velocity measurements made within Congo and neon tetra schools are compared to each other and, in addition, are compared to background noise levels measured in quiescent water in Table 4–4. Notably, it seems that despite having twice the level of abundance, the neon tetras generate turbulence with RMS velocities that are up to an order of magnitude smaller than the those of the Congo tetras. This suggests that body size may be a more important factor in turbulence production than other factors such as abundance, particularly given the fact that qualitative observations of animal behaviour for both the Congo and neon tetras were generally consistent throughout the experiments referenced in this species comparison. Specifically, fish swam at low to moderate cruising speed (that which can be maintained indefinitely) with relatively few observed instances of escape speeds (which can be sustained for short-duration, evasive or predatory manoeuvres), in generally random trajectories of moderate length, within a school located directly below the probe head. Additionally, given that the magnitude of the velocities measured for the neon tetras was close to that due to noise, these specific results might suggest that velocity signals produced by the neon tetras are indistinguishable from those of the instrument noise. Such a low signal to noise ratio (not to be confused with the SNR measured by the ADV) may represent a lower limit in terms of the smallest characteristic animal size and swimming speeds which can be accurately studied using ADVs.

Comparisons between the tetra species as well as between the neon tetras and background noise are also made with regard to the PDFs of the fluctuating w-component of velocity, in

Velocity Component [m s^{-1}]	Congo Tetras	Neon Tetras	Background Noise
W	-2.2×10^{-3}	-2.1×10^{-3}	-1.8×10^{-3}
u_{rms}	1.4×10^{-2}	1.5×10^{-3}	1.1×10^{-3}
v_{rms}	1.3×10^{-2}	1.7×10^{-3}	1.1×10^{-3}
w_{rms}	6.1×10^{-3}	1.1×10^{-3}	7.0×10^{-4}

Table 4–4: Comparison of velocity components measured within schools of Congo tetras and neon tetras, at abundances of 1250 and 2500 animals/m^3, respectively, with measurements of background noise of the Single-point Vectrino in a quiescent, seeded tank.

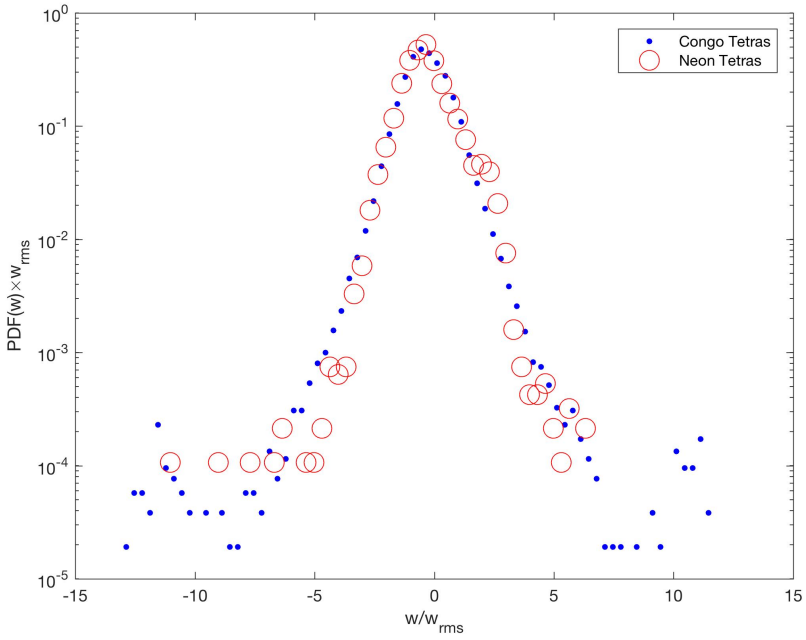

Figure 4–7: Comparison of the normalized PDFs of the fluctuating w-component of velocity, measured within Congo tetra and neon tetra schools, at abundances of 1250 and 2500 animals/m^3, respectively.

Figures 4–7 (normalized) and 4–8, respectively. From the normalized plot, both species produce PDFs with a similar, approximately Gaussian shape, though in dimensional terms the PDF corresponding to the Congo tetras would exhibit a larger spread, given the associated larger values of RMS velocity. Despite the low signal to noise ratios implied by Table 4–4, the neon tetras produce a velocity signal which is clearly different from that of the background noise. While the noise PDF is nearly uniform over a range of ± 4 mm s^{-1}, that corresponding to the neon tetras decays relatively smoothly from its peak at 0 mm/s and beyond the bounds of the noise. Once again, however, the neon tetras at this abundance possibly represent a lower limit of the signal strength of biogenic turbulence that can be captured by the Single-point Vectrino, if the corresponding PDF would narrow any further at lower abundances. This issue must be taken into consideration for future studies, particularly field measurements where the characteristic animal sizes, spacing and swimming speeds may be near such a limit (for

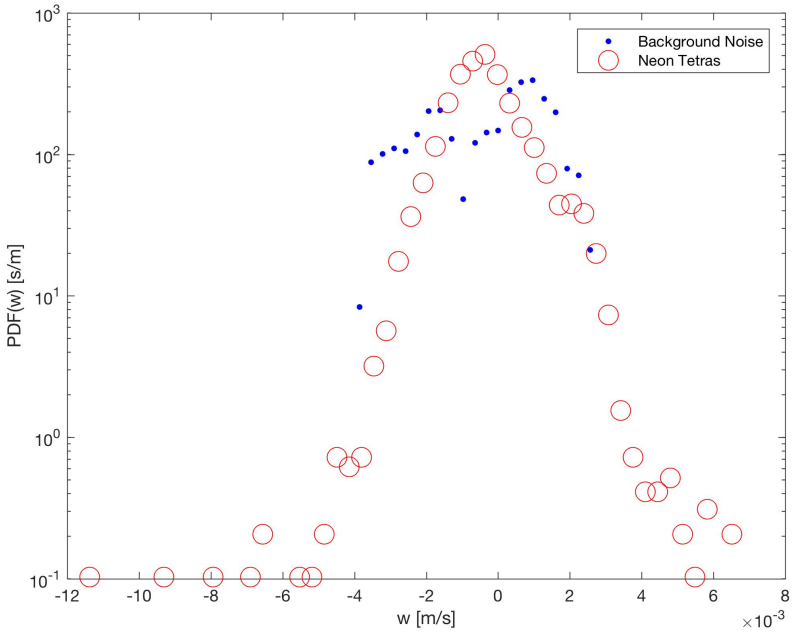

Figure 4–8: Comparison of the PDFs of the fluctuating w-component of velocity, due to background noise and a neon tetra school of 2500 animals/m^3, respectively.

example, in past experiments with small krill [Kunze et al., 2006] or fish at low abundance [Lorke and Probst, 2010]), or not readily observable, due to the nature of such experiments.

The correlation between body size and turbulence production is further illustrated in Table 4–5, where the dissipation rates measured within the two schools of tetra are compared to those of two relatively well-defined experimental results from the literature. Dissipation estimates from field measurements (described in Section 1.3) were not included in this comparison, due to a lack of knowledge regarding the characteristics of the animals contributing to these turbulence measurements. Overall, the present results do not align with the the-

Source	ϵ [W kg^{-1}]	Body length [cm]	Reference
Daphnia magna	$O(10^{-6})$	0.32	[Wickramarathna et al., 2014]
neon tetras	$O(10^{-6})$	3-4	Current work
Congo tetras	$O(10^{-5})$	5-8	Current work
Japanese sardine	$O(10^{-5} - 10^{-4})$	17.3	[Tanaka et al., 2017]

Table 4–5: Comparison of biogenic turbulence dissipation rates between current work and previous studies, listed in order of increasing approximate body length.

oretical predictions of Huntley and Zhou (2004), which, again, assert that dissipation rate should be independent of body size and consistently be $O(10^{-5})$ W kg^{-1} for animals at a natural abundance level. However, the fact that the two smallest species induce dissipation rates of the same order of magnitude ($O(10^{-6})$ W kg^{-1}), but lower than those of the two larger species, which overlap ($O(10^{-5} - 10^{-4})$ W kg^{-1}), gives some support to the theoretical analysis of Huntley and Zhou (2004), but suggests other biological factors to be accounted for. As an example, *Daphnia* do not use the same swimming mechanism as the fish they are compared to and the Japanese sardines exhibited more complex behaviours, such as escape manoeuvres, in the result presented. How these effects can be better accounted for in future biogenic turbulence models and empirical relationships, will depend on the results of more extensive studies, particularly those examining wider ranges of body sizes, swimming mechanisms, and characteristic behaviours. In addition, these results do not consider the effect of the physical constraints on the animals (i.e. tank size) which may affect swimming motions and by extension turbulence production. A more representative analysis may have been achieved by dynamically following the animal aggregations with the measurement device in a tank large enough to consider the school to be unconstrained, however the implementation of such a system was beyond the scope of this study. Regardless of the several unanswered questions pertaining to collective and individual behaviour, body size and morphology, the results above demonstrate that within a stationary school of fish not exhibiting complex and/or highly energetic behaviours (such as predator-prey interactions, diel vertical migration, etc.), aquatic animals ranging in size from that of neon to Congo tetras can induce substantial dissipation rates, and, in the latter case, over a wide range of abundance.

4.3 Comparison with oceanic turbulence data

Lastly, velocity and dissipation measurements from both tetra species are presented in the context of physical processes which are known contributors to mixing and energy dissipation in the ocean. Table 4–6 compares horizontal and vertical RMS velocities measured within the tetra schools to those measured at two depths below the surface of Lake Ontario.

Source (depth)	u_{rms} [m s^{-1}]	w_{rms} [m s^{-1}]	Reference
Congo tetras	7.2×10^{-3}	6.2×10^{-3}	Current work
neon tetras	1.5×10^{-3}	1.1×10^{-3}	Current work
Wind (0.82 m)	7.68×10^{-2}	1.006×10^{-1}	[Kitaigorodskii et al., 1983]
Wind (4.88 m)	2.51×10^{-2}	3.67×10^{-2}	[Kitaigorodskii et al., 1983]

Table 4–6: Comparison of current biogenic turbulence values of horizontal and vertical RMS velocities with those induced primarily by surface winds of 5.8 m s^{-1}, at two depths. The Congo tetra u_{rms} value has been corrected using the method of Khorsandi et al. (2012), assuming isotropy.

Perhaps somewhat unsurprisingly, the velocities induced by the swimming of small fish are an order of magnitude lower than those due to wind and waves near the surface of a lake on a windy day. As importantly, even for extreme cases of violent predation behaviour, where induced velocities may be comparable to those of strong winds, the horizontal length scales of animal aggregations will be substantially smaller than those of large weather events. However, the fact that wind induced RMS velocities decay by roughly 60% within 4 metres of depth, suggests the potential importance of biogenic turbulence, to mixing and dissipation processes, at ocean depths below the (relatively thin) surface mixed layer or in locations with rare wind-forced mixing events.

Dissipation rate measurements are also compared with various values corresponding to physical processes, for multiple surface wind speeds and within different layers of the ocean in Table 4–7. Near the surface, biogenic dissipation rates are below the order of magnitude of those due to wind, and again would generally result in much smaller horizontal length scales than wind forcing. At a depth of approximately 10 m, however, the Congo tetra dissipation rate is an order of magnitude greater than that due to gale force winds, which is also of the same order as that due to the neon tetras. Although, once again, a typical gale would influence much larger length scales, biogenic turbulence may be much more persistent in locations where such weather events are rare. In addition to local dependencies, the range of values corresponding to the contribution of Brainerd and Gregg (1995) demonstrate the seasonal variability of dissipation rates. These measurements, attributed to internal, physical

Source (depth)	ϵ [W kg^{-1}]	Reference
Congo tetras	$O(10^{-5})$	Current work
neon tetras	$O(10^{-6})$	Current work
6-11 m s^{-1} wind (upper 1 m of ocean)	$O(10^{-4})$	[Kitaigorodskii et al., 1983]
5 m s^{-1} wind (upper 10 m of ocean)	1.4×10^{-7}	[MacKenzie and Leggett, 1993]
20 m s^{-1} wind (upper 10 m of ocean)	8.5×10^{-6}	[MacKenzie and Leggett, 1993]
internal processes (top of pycnocline)	$O(10^{-9} - 10^{-6})$	[Brainerd and Gregg, 1995]
internal processes (mixed layer)	$O(10^{-7} - 10^{-5})$	[Brainerd and Gregg, 1995]

Table 4–7: Comparison of current measurements of biogenic turbulence dissipation rates with those of physical processes in the ocean.

processes in the open ocean are typical of the range of dissipation rates observed over the course of a year in two characteristic fluid layers of the ocean. The fact that the tetra-induced dissipation rates are at the upper end of these ranges is certainly intriguing, and demonstrates the importance of accounting for or potentially correlating seasonal animal presence and behaviours with the extent of expected biogenic contributions to mixing in a particular area of the ocean. However, it should be recalled that the tetra experiments were carried out in an unstratified fluid environment as opposed to the stratified pycnolcline and thermocline, where biogenic turbulence may be of the most importance according to the previous data comparisons. In discussing the role of biogenic turbulence in stratified regions of the ocean, the corresponding length scales must be compared to values of buoyancy and overturning length scales (i.e. the Ozmidov and Thorpe scales, respectively [Thorpe, 2005]) typical of a given region of interest in the ocean. It should be noted that integral length scales of the biogenic turbulence produced by the Congo tetras (given by $L = \tau w_{rms}$) are of $O(10^{-4} - 10^{-3})$ m and that the largest possible induced fluid motions produced by an individual should not greatly exceed the order of magnitude of the animals body size ($O(10^{-2})$ m). Furthermore, this range of values is near the lower end of typically observed values of both the Ozmidov and Thorpe scales ([Dillon, 1982]). Therefore, these scales may be limiting factors when it comes to identifying species, behaviours, and conditions conducive to substantial biogenic mixing.

These wind-based results do not necessarily account for the effects of other processes, such as wave breaking or wake generation near topographic features, which may increase dissipation rates. This, however, does not diminish the potential significance of the biogenic turbulence results, but merely adds complexity to the problem of identifying locations where and conditions in which biogenic turbulence may be either a dominant or a non-negligible flow feature. Biogenic turbulence may be even more important within regions of high stratification, where the background dissipation rate may be as much as 4 to 6 orders of magnitude lower than that resulting from fish ranging in size from that of the neon tetras to Congo tetras, respectively, so long as the animal-induced fluid motions are of sufficient size and energy. Importantly, these regions may be traversed by animals undergoing diel vertical migration, which, as shown by Hooper et al. (2016), may lead to increased dissipation rates as compared to those of the stationary aggregations in the present study. Furthermore, such migrations may lead to aggregation-scale vertical fluid motions, as described by Wilhelmus and Dabiri (2014), which may contribute to enhanced vertical mixing as compared with that due solely to physical processes.

From a fundamental perspective, biogenic turbulence has been shown to exhibit approximate isotropy, as well as velocity PDFs and spectra consistent with those observed in physically-forced turbulence. Furthermore, controlled, behaviourally simple, experiments have demonstrated a potential relationship between animal size and turbulence parameters as well as a lack of dependence of turbulence parameters on abundance, over the ranges investigated. Finally, comparisons of the current experimental results with those typical of measurements in the ocean, suggest the potential importance of biogenic turbulence to mixing and dissipation, particularly in regions with low wind forcing, or at depths below the influence of surface winds with sufficiently small buoyancy and overturning scales. Although the results presented were made in a controlled, repeatable manner, and with a validated measurement technique, experiments involving animals are inherently subject to unique and often unpredictable uncertainties, as discussed in the following chapter.

CHAPTER 5
Sources of error

Several factors have contributed to uncertainty in the results, including, instrument resolution, data filtering methods, and behavioural inconsistencies of the fish. While these aspects affect the results to different degrees and in different manners, none are thought to have compromised the accuracy of the results on an order of magnitude basis. The first question is whether or not the Single-point Vectrino can adequately resolve the smallest scales (the Kolmogorov microscales) of the flow, both spatially and temporally. The Kolmogorov microscales of length and time, as defined in Equation 1.11 are estimated in Table 5–1 for the two tetra species, using the order of magnitude results of Table 4–5 and a kinematic viscosity of 10^{-6} m^2 s^{-1}. The Single-point Vectrino samples at 25 Hz (or once every 0.04 s)

Species	η [mm]	τ [s]
Congo tetra	0.3	0.1
neon tetra	1	1

Table 5–1: Estimates of the Kolmogorov microscales of length and time, respectively, corresponding to the turbulence produced by each species of tetra.

and therefore should be able to accurately capture the smallest time scales of the biogenic turbulence under investigation, which are approximately $1 - 2$ orders of magnitude larger than the instrument resolution. The Kolmogorov length scale of both species' turbulence, however, is smaller than either dimension of the Single-point Vectrinos sampling volume (6 mm in diameter and 3-15 mm in height). The lack of the ADVs ability to fully resolve the smallest length scales would generally lead to underestimates of the dissipation rate, however, because the biogenic dissipation rate is estimated using large scale quantities (w_{rms} and T), this source of error should not appreciably affect the order of magnitude results.

Secondly, it is possible that the method of filtering the data, to exclude instances of fish within the sampling volume of the ADV, has erroneously removed points for which there was significant acoustic interference from fish in close proximity to the ADV transducers, though not in the sampling volume. Assuming that such data points would likely correspond to relatively large velocity fluctuations, since vortex and wake velocities should be highest close to the fish producing them, this unintended excision of data would serve to underestimate the true RMS velocities and dissipation rates. It is also possible that this issue is exacerbated at higher abundance levels, due to the higher probability that a fish will be close enough to the transducers to contaminate a reading at any given time. In addition to the effects resulting from fish being extremely close to the ADV transducers, there is also the fact that having a large number of solid objects moving around the tank, in this case fish, will lead to lower overall SNR levels. This is due to boundary-type echoes off of fish throughout the tank which may contaminate the desired reflections from within the sampling volume. This potential, overall decrease in SNR would increase the likelihood of normal fluctuations in SNR dropping below the filtering threshold, and, combined with the previously described over-filtering, reduce the measured RMS velocities and dissipation rates. Furthermore, the effects of boundary echo interference due to the presence of fish may be related to abundance, as fish would be more likely to be in a location and orientation to facilitate such echoes at higher abundances. Finally, as a practical consideration, by leading to increased data loss, these two sources of error are likely to have increased the sampling time required to obtain converged turbulence statistics, as compared to laboratory measurements without the presence of animals.

Moreover, the fact that the stationary ADV is an Eulerian time measurement device, whereas the integral time scale used in the estimate of the dissipation rate is ideally Lagrangian, will affect the biogenic turbulence results in a similar manner to that noted for the jet validation measurements described in Chapter 3. As it is possible that the Eulerian time scale is shorter than its Lagrangian equivalent (though they are assumed to be equal in

this work), the dissipation rates presented may be further overestimated, though this effect should be partially mitigated by the choice of C_{ϵ_2}. However, because the constant of proportionality between the two should be of order unity, the order of magnitude of the dissipation results should remain as stated. Even less clear, though related to the ADV, is the effect that acoustic streaming may have had on the results. For instance, it may be possible that the addition of the mean flow away from the ADV probe head has made vertical motions more persistent, thus increasing the corresponding integral time scale (and decreasing the dissipation rate) as well as suppressing the fish-induced fluid motions in general, potentially leading to reduced RMS values. Any error contributions to the biogenic turbulence results due to slight misalignments of the ADV probes, are likely minimal, given the approximate isotropy of the flow discussed in Section 4.1, and could even partially explain the small discrepancy between the values of Table 4–1. Furthermore, the effect of any slight decrease in water temperature (which is measured by the ADVs at the beginning of each experiment) is likely minimal given the $\ll 1\%$ difference between sound speeds at, for example, 26 and 28°C [Grosso and Mader, 1972].

Finally, it is possible that variations in behaviour, such as aggregation structure and swimming speed, which were not detected in the simple qualitative observations of the experiments, affected the reported integral time scales and dissipation rates. Although turbulence statistics were converged at each abundance for example, it is unclear whether the hypothetical explanations for the order of magnitude consistency of results over the abundance range, can sufficiently describe this phenomenon, or if there are more complex factors at play which could only be quantified with extensive and systematic behavioural analyses. However, given the convergence of the data, it is unlikely that these or any other biological factors would change the general result that Congo tetras induce dissipation rates of $O(10^{-5})$ W kg^{-1}.

In general, the reason that the results of this work are presented most often on an order of magnitude basis, is due to the fact that the sources of error discussed above are difficult to quantify, particularly within the scope of this project. However, the controlled manner

in which these experiments were conducted has eliminated many of the error-causing variabilities inherent to ocean measurements, thus providing a higher level of confidence in these measurements than those of many past experiments. Furthermore, the order of magnitude quantification of biogenic turbulence may be sufficient in many applications, such as ocean energy budget calculations, in which the contributions of physical processes are only known to within orders of magnitude [Ferrari and Wunsch, 2009]. Given that the several factors contributing to potential underestimates of dissipation rate, particularly those related to the spatial resolution of the Single-point Vectrino and over-filtering of data, are, to some extent, potentially counteracted by those of data segment length limitations and integral time scale underestimates, the orders of magnitude of the dissipation rates presented should not be affected. As well, the several other contributions to experimental uncertainty from ADV functionality and biological factors are deemed to be both small, and have been limited as much as possible given the consistency with which the experimental procedure was undertaken for every measurement, as well as the convergence of the data presented. The accurate quantification of these sources of error will be crucial in future studies, with the goal of precisely defining models of biogenic turbulence which incorporate a wide range of physical and biological parameters. As discussed in the following chapter, the possibility of tracking individual animals during similar experiments will serve to better validate the current data-filtering method and allow for the statistical analysis of animal behaviour.

CHAPTER 6
Conclusions

Over the course of this project, the apparatus and procedures for a systematic investigation of biogenic turbulence, produced by two species of small fish in a controlled environment, have been developed and carried out while adhering to the ethics protocols of the UACC. In addition, a turbulent jet apparatus was constructed and subsequently used to characterize the performance of two ADVs. The results of the biogenic turbulence experiments have been presented and discussed in the context of the general structure of biogenic turbulence, the effects of biological factors on turbulence parameters, and the relative energetics of biogenic turbulence compared to those associated with physical oceanic processes. The sources of uncertainty associated with the aforementioned results, stemming from data analysis, instrumentation, and biology have also been addressed in a predominately qualitative manner. Overall, this work has shed light on a potentially important phenomenon contributing to fluid dynamical processes throughout the world's oceans, and has provided a multitude of potential objectives for future studies, as detailed below.

6.1 Experimental results

In an effort to better inform the debate over the relative significance of biogenic turbulence to oceanic processes, an experimental procedure was developed in which turbulence measurements could be made within schools of small fish under controlled laboratory conditions. First, two species of hardy, naturally schooling species of fish, namely, neon tetras and the larger Congo tetras, were selected as research subjects, given the similarity of many biological characteristics to those of previously studied marine species. Subsequently, an animal use protocol (Protocol #2014-7505) was developed in conjunction with the UACC encompassing the experimental and everyday treatment of the animals, both during and after the conclusion of this study. With regard to the experiments themselves, the use of two species

of fish allowed for the investigation of the effects of body size on turbulence production, while the variation in enclosure volume allowed for the effects of animal abundance to be studied. The experimental set-up, including seeding of the water for proper ADV functionality, was performed while minimizing any effects on animal behaviour that could potentially affect the integrity of the data. Efforts were also devoted to the filtering of velocity time series, so as to remove data points corresponding to the presence of fish in the ADV sampling volume, without artificially biasing the resulting statistics. This filtering method however, necessitated the development of custom MATLAB codes for the analysis of the resulting gappy time series. Through the acquisition of extensive experience caring for and working with animals as well as the refinement of measurement and data analysis techniques over the course of this project, a robust experimental procedure was established and could easily be replicated with, or adapted to future experiments involving the lab-based measurement of biogenic turbulence induced by other species using ADVs.

Further to the development of the above methodology, the performance of two ADVs, the more established Single-point Vectrino and the more recent, and advanced, Vectrino Profiler, have been benchmarked in experiments along the axis of a turbulent jet. Specifically, the comparison of mean and RMS velocity measurements, turbulent velocity PDFs and spectra, as well as estimates of the dissipation rate, between the two ADVs and with accepted results, in the literature, have validated the ability of the Vectrino Profiler to accurately measure turbulent flows, albeit with somewhat higher levels of signal noise than the standard Single-point Vectrino. In particular, the instruments reproduced the expected $(x/D)^{-1}$ downstream decay of mean axial velocity and the asymptotic downstream evolution of RMS velocities (particularly with the z-beam of the ADVs). Approximately Gaussian velocity PDFs and spectra exhibiting the theoretical -5/3 slope of decay were also best obtained using the z-beam of each ADV. Finally, the downstream evolution of dissipation rate, as measured more directly by the Vectrino Profiler, and estimated from large-scale quantities, by the Single-point Vectrino, demonstrated the accepted $(x/D)^{-4}$ trend. The fact that the Single-point

Vectrino was shown to be capable of accurately estimating the dissipation rate using large scale quantities, namely the RMS velocity and the integral time scale, was an additional valuable result, in and of itself, given this instrument's common use in oceanic turbulence experiments. This separate validation study has also helped establish these two Nortek Vectrino ADVs as suitable measurement devices for the study of turbulent flows, including present and future research related to biogenic turbulence.

The subsequent, direct measurements of biogenic turbulence have allowed for the characterization of this phenomenon, especially as it relates to classic turbulence theory. Moreover, the effects of animal abundance and body size on turbulence production, including the limitations of the Single-point Vectrino related to measuring turbulence produced by the smallest fish have been investigated. Finally, these controlled laboratory results have been compared to those of past biogenic turbulence studies and characteristic levels of background turbulence in the ocean, attributed to physical processes. Specifically, the turbulence produced within a school of Congo tetras at moderately high abundance was shown to be approximately isotropic within stationary animal aggregations, thereby validating this assumption, found in much of the existing literature, and simplifying current and future analyses. Additionally, the PDFs of the fluctuating velocity component exhibited an approximately Gaussian form and the frequency spectrum of fluctuating velocity exhibited slopes consistent with the -5/3 theoretical prediction in the inertial subrange, both indicative of a similarity with conventional, physically forced turbulence. This consistency with turbulence theory justifies the application of established analytical tools to the developing field of biogenic turbulence research, which may aid in accelerating the advance of the understanding of its nature and significance in oceanic processes. As mentioned, experiments performed with the Congo tetra school exhibited no clear relationship between the abundance and the measured turbulence parameters (over the span of abundances investigated), potentially due to behavioural variations related to animal spacing. Dissipation rates corresponding to the neon tetras were found to be an order of magnitude lower than theoretical predictions, while those corresponding to

Congo tetras were approximately an order of magnitude higher, in contrast to the independence of dissipation rates on body size postulated by Huntley and Zhou (2004). However, the neon tetras were found to produce dissipation rates similar to those of the much smaller *Daphnia magna*, while dissipation rates in the Congo tetra school were at or above values within schools of the larger Japanese sardines. These results demonstrate the complexity of biogenic turbulence and suggest other behavioural and morphological factors will affect turbulence energetics, in addition to body size. Finally, RMS velocities and dissipation rates within the fish aggregations we up to an order of magnitude lower than those typical of the upper 5 m of the ocean, when subjected to surface winds between approximately 5 and 20 m s^{-1}. However, the biogenic dissipation rates were at or above those found at approximately 10 m depth and up to 6 orders of magnitude greater than those found in regions of strong stratification. Therefore, at local scales, such biogenic turbulence may contribute substantially to mixing and energy dissipation in the absence of large-scale physical processes, and perhaps further, in cases of more energetic behaviours such as DVM and predator-prey interactions. Although, the impact of biogenic turbulence will also be restricted by relevant buoyancy and overturning scales in stratified regions and seasonal changes to the luid environment. Given these observations, biogenic turbulence is a complex process with a potentially important role in both localized marine ecosystems and global ocean circulation, which will require continued, comprehensive research to better understand the factors governing its nature and significance.

6.2 Future work

As demonstrated throughout this work, biogenic turbulence is both an intriguing and complex phenomenon, and while the results of this study have helped to better inform the debate over its relative significance in the ocean, they have also presented a multitude of questions to be answered by way of future research. To provide a clear understanding of the role of biogenic turbulence, successive investigations should broadly address several topics. First, the investigation of biological factors (including morphology and behaviour) using a

variety of measurement techniques. Second, identifying locations where biogenic turbulence may play a non-negligible role in mixing processes and making rigorous field observations at such locations. And, finally, using the results of the aforementioned research to construct empirical models for the prediction of biogenic turbulence parameters and their incorporation into physical descriptions of oceanic processes such as energy budgets and circulation models.

The biological factors which may impact biogenic turbulence are extraordinarily varied. For example, the effects of variations in body size, swimming speed and aggregation structure, morphology and swimming mechanism, migration behaviour, and others are likely inter-related and have an impact on the structure and energetics of biogenic turbulence. The most logical first step in the continuation of this research would be to implement a larger variety of species, but of similar morphology and behaviour to the tetras, into the present experimental procedure. Gathering data over a wider range of animal sizes would serve to better define the correlation between size (and by extension, Reynolds number) with turbulence generation, all while maintaining simple behaviour in a stationary school. Such measurements could be made with other species of tetra (of the *Characidae* family, specifically), as well as expanded to some of the more readily available Clupeiforme species, such as Atlantic herring, which correspond to the small and mid-sized species considered in the predictions of Huntley and Zhou (2004). By focusing sets of experiments on individual biological families, the effects of morphology and swimming mechanism can be isolated as much as possible from the effect of body size.

The incorporation of three-dimensional tracking of the animals into the procedure described in Chapter 2 would allow for the quantification of any effects of swimming speed and aggregation structure on turbulence production, as well as their relationship to abundance, across the range of species under investigation. Furthermore, lab-based observations could be compared to ocean observations for behavioural consistency, and used for the validation of existing models of abundance and aggregation structure in biogenic turbulence estimates

[Makris et al., 2006, Huntley and Zhou, 2004]. In addition, 3-D tracking would allow for estimates of the kinetic energy of individual animals and the corresponding aggregation, which could then be compared to the measured TKE, so as to better understand the efficiency with which aquatic animals generate turbulence. Finally, similarly-sized species with known differences in swimming speed and aggregation structure could be compared to elucidate the effect of these parameters on biogenic turbulence, thereby allowing for the more accurate prediction of turbulence production based on existing species biomass, behaviour, and distribution data.

Such experiments could also be extended to animals of both differing morphology and different swimming mechanisms, for example, shrimp, krill, and jellyfish, all of which are known to form large aggregations in the ocean. Gathering such a diverse array of data would result in more accurate predictions of the extent biogenic turbulence by allowing models and scaling to be tailored to more specific species, as well as enabling the better identification of species and conditions corresponding to significant biogenic turbulence for further study. The apparatus and procedure of this study could also be modified to study more complex behaviours in aquatic animals, after a satisfactory amount of baseline measurements have been made. For example, by conducting experiments while animals are feeding as well as while they are migrating vertically through a water column, a more precise estimate of the biogenic turbulence can be made by including the possibly elevated levels of turbulence exhibited throughout the behavioural cycles of animals, whether daily, in the case of DVM, or seasonal, such as large scale migrations and spawning activities. By also performing these measurements in stratified water columns, and/or measuring such parameters as temperature, salinity, and nutrient concentrations throughout the experimental enclosure, a better understanding of biogenic turbulence driven vertical mixing, including mixing efficiency, aggregation scale flow structures [Wilhelmus and Dabiri, 2014], and nutrient distribution could be developed. Such information would not only be useful in describing the importance of

the effects of animals on overturning circulation in the ocean, but also aid in the design of aquaculture enclosures and husbandry techniques, further to the results of Plew et al. (2015).

Ideally, such experimental data may be used to construct predictive models for the energetics and impacts of biogenic turbulence using the above biological parameters and current estimates of animal biomass and distribution in the ocean. Combined with weather and ocean current data, these predictions could be used to identify locations at which biogenic turbulence may be a non-negligible contributor to mixing and where field measurements should be carried out for comparison with laboratory results. However, such field measurements should, as much as possible, encompass observations of the biological parameters mentioned above for accurate validation. Additionally, observations of previously unknown or neglected animal populations such as those described by Irigoien et al. (2014) should also include turbulence measurements, wherever possible, so as to acquire much needed biological and turbulence data associated with those less explored species and regions of the ocean. Ultimately, having established relationships between biological factors and biogenic turbulence, and using up to date wildlife observations, the contribution of biogenic turbulence to the ocean energy budget can be determined, along with the precise role of biogenic turbulence in ocean circulation. Where available, historical biomass data could also be used to determine the possible extent to which humans have disrupted oceanic processes through overfishing and habitat destruction.

The construction of such an extensive understanding of the nature and impacts of biogenic turbulence remains, admittedly, a daunting task; however, through extending this experimental procedure to a more diverse range of marine species and behaviours with additional measurement devices, performing more rigorous field measurements and observations, and finally, using biomass, behaviour, and distribution data to scale controlled laboratory measurements, sufficiently accurate estimates of the significance of biogenic turbulence in the global ocean may be obtained. In the end, our comprehension of the role and nature of biogenic turbulence is but one small, yet important, chronicle on a voyage of scientific

exploration, embarked upon by Darwin, Cousteau and countless others, toward a deeper knowledge of the biosphere, ocean, global climate, and their interconnections, especially the impacts of humans affecting the environment in which we live.

REFERENCES

[Antonia et al., 1980] Antonia, R., Satyaprakash, B., and Hussain, A. (1980). Measurements of dissipation rate and some other characteristics of turbulent plane and circular jets. *Physics of Fluids*.

[Ardekani and Stocker, 2010] Ardekani, A. and Stocker, R. (2010). Stratlets: low reynolds number point-force solutions in a stratified fluid. *Physical review letters*.

[Brainerd and Gregg, 1995] Brainerd, K. and Gregg, M. (1995). Surface mixed and mixing layer depths. *Deep-Sea Research I*.

[Brand et al., 2016] Brand, A., Noss, C., Dinkel, C., and Holzner, M. (2016). High-resolution measurements of turbulent flow close to the sediment-water interface using a bistatic acoustic profiler. *Journal of Atmospheric and Oceanic Technology*.

[Burden and Faires, 2011] Burden, R. and Faires, J. (2011). *Numerical Analysis*. Brooks/Cole, 9th edition.

[Camozzi, 2015] Camozzi, S. (2015). Quantification of biogenic turbulence.

[Corrsin, 1963] Corrsin, S. (1963). Estimates of the relations between eulerian and lagrangian scales in large reynolds number turbulence. *Journal of the Atmospheric Sciences*.

[Craig et al., 2011] Craig, R., Loadman, C., Clement, B., Rusello, P., and Siegel, E. (2011). Characterization and testing of a new bistatic profiling acoustic doppler velocimeter: The vectrino-ii. In *Proceedings of the IEEE/OES/CWTM Tenth Working Conference on Current Measurement Technology*.

[Darwin, 1953] Darwin, C. (1953). Note on hydrodynamics. *Mathematical Proceedings of the Cambridge Philosophical Society*.

[Dean et al., 2016] Dean, C., Soloviev, A., Hirons, A., Frank, T., and Wood, J. (2016). Biomixing due to diel vertical migrations of zooplankton: Comparison of computational fluid dynamics model with observations. *Ocean Modelling*.

[Dewar et al., 2006] Dewar, W., Bingham, R., Iverson, R., Nowabek, D., St Laurent, L., and Wiebe, P. (2006). Does the marine biosphere mix the ocean? *Journal Of Marine Research*.

[Dillon, 1982] Dillon, T. (1982). Vertical overturns: A comparison of thorpe and ozmidov length scales. *Journal of Geophysical Research*.

[Emery and Thomson, 2004] Emery, W. and Thomson, R. (2004). *Data analysis methods in physical oceanography*. Elsevier, 2nd and revised edition.

[Ferrari and Wunsch, 2009] Ferrari, R. and Wunsch, C. (2009). Ocean circulation kinetic energy: Sources and sinks. *Annual Review of Fluid Mechanics*.

[Ferrari and Wunsch, 2010] Ferrari, R. and Wunsch, C. (2010). The distribution of eddy kinetic and potential energies in the global ocean. *Tellus*.

[García et al., 2005] García, C., Cantero, M., Niño, Y., and Garcia, M. (2005). Turbulence measurements with acoustic doppler velocimeters. *Journal of Hydraulic Engineering*.

[Goring and Nikora, 2002] Goring, D. and Nikora, V. (2002). Despiking acoustic doppler velocimeter data. *Journal of Hydraulic Engineering*.

[Gourdon, 2009] Gourdon, J. (2009). *SOP 519.01 - Aquatic Animal Husbandry*. Comparative Medicine and Animal Resources Centre. McGill University.

[Gregg and Horne, 2009] Gregg, M. and Horne, J. (2009). Turbulence, acoustic backscatter, and pelagic nekton in monterey bay. *Journal Of Physical Oceanography*.

[Grosso and Mader, 1972] Grosso, V. and Mader, C. (1972). Speed of sound in pure water. *The Journal of the Acoustical Society of America*.

[Hooper et al., 2016] Hooper, V, J., Baringer, M., St Laurent, L., Dewar, W., and Nowacek, D. (2016). Dissipation processes in the tongue of the ocean. *Journal of Geophysical Research: Oceans*.

[Huntley and Zhou, 2004] Huntley, M. and Zhou, M. (2004). Influence of animals on turbulence in the sea. *Marine Ecology Progress Series*.

[Hussein et al., 1994] Hussein, H., Capp, S., and George, W. (1994). Velocity measurements in a high-reynolds-number, momentum-conserving, axisymmetric, turbulent jet. *Journal of Fluid Mechanics*.

[Irigoien et al., 2014] Irigoien, X., Klevjer, T., Røstad, A., Martinez, U., Boyra, G., Acuña, J., Bode, A., Echevarria, F., Gonzalez-Gordillo, J., Hernandez-Leon, S., Agusti, S., Aksnes, D., Duarte, C., and Kaartvedt, S. (2014). Large mesopelagic fishes biomass and trophic efficiency in the open ocean. *Nature*.

[Katija, 2012] Katija, K. (2012). Biogenic inputs to ocean mixing. *The Journal of Experimental Biology*.

[Katija, 2015] Katija, K. (2015). Morphology alters fluid transport and the ability of organisms to mix oceanic waters. In *Integrative and Comparative Biology*, volume 55.

[Katija and Dabiri, 2008] Katija, K. and Dabiri, J. (2008). In situ field measurements of aquatic animal-fluid interactions using a self-contained underwater velocimetry apparatus (scuva). *Limnology and Oceanography: Methods*.

[Katija and Dabiri, 2009] Katija, K. and Dabiri, J. (2009). A viscosity-enhanced mechanism for biogenic ocean mixing. *Nature*.

[Khorsandi et al., 2012] Khorsandi, B., Mydlarski, L., and Gaskin, S. (2012). Noise in turbulence measurements using acoustic doppler velocimetry. *Journal of Hydraulic Engineering*.

[Kitaigorodskii et al., 1983] Kitaigorodskii, S., Donelan, M., Lumley, J., and Terray, E. (1983). Wave-turbulence interactions in the upper ocean. part ii. statistical characteristics of wave and turbulent components of the random velocity field in the marine surface layer. *Journal of Physical Oceanography*.

[Kunze, 2011] Kunze, E. (2011). Fluid mixing by swimming organisms in the low-reynolds-number limit. *Journal of Marine Research*.

[Kunze et al., 2006] Kunze, E., Dower, J., Beveridge, I., Dewey, R., and Bartlett, K. (2006). Observations of biologically generated turbulence in a coastal inlet. *Science*.

[Lhermitte and Serafin, 1984] Lhermitte, R. and Serafin, R. (1984). Pulse-to-pulse coherent doppler sonar signal processing techniques. *Journal of Atmospheric and Oceanic Technology*.

[Liljebladh and Thomasson, 2001] Liljebladh, B. and Thomasson, M. (2001). Krill behaviour as recorded by acoustic doppler current profilers in the gullmarsfjord. *Journal of Marine Systems*.

[Lorke and Probst, 2010] Lorke, A. and Probst, W. (2010). In situ measurements of turbulence in fish shoals. *Limnology and Oceanography*.

[MacKenzie and Leggett, 1993] MacKenzie, B. and Leggett, W. (1993). Wind-based models for estimating the dissipation rates of turbulent energy in aquatic environments: empirical comparisons. *Marine Ecology Progress Series*.

[Makris et al., 2006] Makris, N., Ratilal, P., Symonds, D., Jagannathan, S., Lee, S., and Nero, R. (2006). Fish population and behavior revealed by instantaneous continental shelf-scale imaging. *Science*.

[Munk, 1966] Munk, W. (1966). Abyssal recipes. *Deep-Sea Research*.

[Nortek, 2004] Nortek (2004). *Vectrino velocimeter, user guide*. Nortek AS.

[Nortek, 2012] Nortek (2012). *Vectrino profiler, profiling velocimeter user guide*. Nortek AS.

[Nortek, 2013] Nortek (2013). *Datasheet Vectrino Lab*. Nortek AS.

[Noss et al., 2013] Noss, C., Dabrunz, A., Rosenfeldt, R., Lorke, A., and Schulz, R. (2013). Three-dimensional analysis of the swimming behavior of daphnia magna exposed to nano-sized titanium dioxide. *PLoS ONE*.

[Noss and Lorke, 2014] Noss, C. and Lorke, A. (2014). Direct observation of biomixing by vertically migrating zooplankton. *Limnology and Oceanography*.

[Plew et al., 2015] Plew, D., Klebert, P., Rosten, T., Aspaas, S., and Birkevold, J. (2015). Changes to flow and turbulence caused by different concentrations of fish in a circular tank. *Journal of Hydraulic Research*.

[Pointdexter et al., 2010] Pointdexter, C., Rusello, P., and Variano, E. (2010). Acoustic doppler velocimeter-induced acoustic streaming and its implications for measurement. *Experiments in Fluids*.

[Pope, 2000] Pope, S. (2000). *Turbulent Flows*. Cambridge University Press.

[Press et al., 1996] Press, W., Teukolsky, S., Vetterling, W., and Flannery, B. (1996). *Numerical Recipes in Fortran 77: The Art of Scientific Computing*, volume 1 of Fortran Numerical Recipes. Cambridge University Press, 2nd edition.

[Rousseau et al., 2010] Rousseau, S., Kunze, E., Dewey, R., Bartlett, K., and Dower, J. (2010). On turbulence production by swimming marine organisms in the open ocean and coastal waters. *Journal Of Physical Oceanography*.

[St Laurent and Simmons, 2006] St Laurent, L. and Simmons, H. (2006). Estimates of power consumed by mixing in the ocean interior. *Journal of Climate*.

[Subramanian, 2010] Subramanian, G. (2010). Viscosity-enhanced bio-mixing of the oceans. *CURRENT SCIENCE*.

[Tanaka et al., 2017] Tanaka, M., Nagai, T., Okada, T., and Yamazaki, H. (2017). Measurement of sardine-generated turbulence in a large tank. *Marine Ecology Progress Series*.

[Taylor, 1935] Taylor, G. I. (1935). Statistical theory of turbulence. In *Proceedings of the Royal Society of London A: Mathematical, Physical and Engineering Sciences*, volume 151, pages 421–444. The Royal Society.

[Tennekes and Lumley, 1972] Tennekes, H. and Lumley, J. (1972). *A First Course in Turbulence*. The MIT Press.

[Thomas et al., 2017] Thomas, R., Schindfessel, L., McLelland, S., Crelle, S., and Mulder, T. (2017). Bias in mean velocities and noise in variances and covariances measured using a multistatic acoustic profiler: the nortek vectrino profiler. *Measurement Science and Technology*.

[Thorpe, 2005] Thorpe, S. (2005). *The Turbulent Ocean*. Cambridge University Press.

[Thorpe, 2007] Thorpe, S. (2007). *An Introduction to Ocean Turbulence*. Cambridge University Press.

[Vassilicos, 2015] Vassilicos, J. (2015). Dissipation in turbulent flows. *Annual Review of Fluid Mechanics*.

[Wang and Ardekani, 2015] Wang, S. and Ardekani, A. (2015). Biogenic mixing induced by intermediate reynolds number swimming in stratified fluids. *Nature*.

[Wickramarathna et al., 2014] Wickramarathna, L., Noss, C., and Lorke, A. (2014). Hydrodynamic trails produced by daphnia: Size and energetics. *PLoS ONE*.

[Wilhelmus and Dabiri, 2014] Wilhelmus, M. and Dabiri, J. (2014). Observations of large-scale fluid transport by laser-guided plankton aggregations. *Physics of Fluids*.

[Wunsch and Ferrari, 2004] Wunsch, C. and Ferrari, R. (2004). Vertical mixing, energy, and the general circulation of the oceans. *Annual Review of Fluid Mechanics*.

[Wygnanksi and Fielder, 1969] Wygnanksi, I. and Fielder, H. (1969). Some measurements in the self-preserving jet. *Journal of Fluid Mechanics*.

[Zedel and Hay, 2011] Zedel, L. and Hay, A. (2011). Turbulence measurements in a jet: Comparing the vectrino and vectrinoii. In *Proceedings of the IEEE/OES/CWTM Tenth Working Conference on Current Measurement Technology*.